High Power Laser System for the Creation of Bose-Einstein Condensations

Vasiliki Bolpasi

A thesis presented for the degree of
Master of Science

Physics Department - University of Crete

IESL - FORTH

2008

High Power Laser System for the Creation of Bose-Einstein Condensations

Vasiliki Bolpasi

A thesis presented for the degree of

Master of Science

2008

Abstract

In this thesis is described the development of a laser system for the creation of Bose-Einstein Condensates (BEC). The requirements for the laser light are explained, and the major components of our laser system are described.

A more detailed description of the amplification of the laser radiation is given to emphasize my contribution to this ongoing project. There are two different configurations presented for the amplification system and study the properties of the resulting beam concerning its power and spectral purity.

The major properties of the amplification system that we describe, are that it can give up to $300mW$ of usable power, coming from a seed beam with power of only $0.5mW$. The design was carefully optimized in order to provide stability and reliability, which are very important principles of a system participating in such complex experiments as those of Bose-Einstein Condensation.

Acknowledgements

The work for this thesis is done in the Cretan Matter Waves laboratory at the Institute of Electronic Structure and Lasers (I.E.S.L. - FO.R.T.H.) in Crete, under the supervision of the leader of the group Wolf von Klitzing. I would like to thank him for his guidance, his help and his support during these two years.

Special thanks to my friends and collaborators, Paul Condylis, for the time that he spent for correcting my thesis, and Daniel Sahagun-Sanchez and Olivier Morizot, for their important contribution on carrying out the present thesis.

Finally the rest of the group, Melina Pappa, Mark Baker, and Grigoris Konstadinidis for their support.

Contents

Chapter 1

Introduction

In 1924 Bose and Einstein made the first theoretical prediction about a new state of matter, where the quantum properties of particles exhibit themselves on a macroscopic scale. More specifically they predicted that below a certain temperature a macroscopic number of boson particles would occupy the lowest energy single particle state. This state of matter was called Bose-Einstein Condensation or BEC. (In this thesis BEC will also refer to Bose-Einstein Condensate). The first experimental observation of a BEC took place 71 years later, in 1995, by Ketterle and Wieman & Cornell [1, 2], who were awarded with the Nobel Prize in Physics in 2001. This achievement created new perspectives for the study of the quantum properties of matter with tremendous consequences on high resolution spectroscopy studies and high precision metrology [3].

The realization of a BEC is the purpose of the Cretan Matter Waves laboratory in Crete (FORTH-IESL). For the creation of a BEC, very low temperatures, of the order of nK, must be achieved. For that reason several cooling and trapping methods must be applied. Two of them are the Magneto-Optical Trap (MOT) and Evaporative Cooling of atoms inside a confining potential. These methods use a combination of magnetic fields and laser radiation. For the laser radiation, certain conditions, concerning the frequency, the power, the polarization, the stability, and the reliability must be fulfilled. In this thesis the development of the laser system which fulfills these requirements is described. The several parts of the laser system are also described, while emphasis is given to the part of the system where the laser radiation is amplified.

The present work is organized as follows: In chapter 2, the manipulation of atoms by laser radiation, for cooling and trapping, is described. We mention the main principles of atom cooling and trapping methods required for our purpose, and the properties of the laser radiation to be used. In chapter 3, there is a description of the several parts of the laser system and in chapter 4, we focus on the amplification of the laser light. Two different configurations for the amplification are presented and the properties of the resulting beam, concerning its power and spectral purity, are studied, and a comparison is made between the two configurations. Finally, in chapter 5 there are the conclusions.

Chapter 2

Manipulating Atoms with Light

In order to make and observe a Bose-Einstein condensate (BEC), several techniques of cooling, trapping, and imaging the atoms are needed. In some cases, these techniques demand the use of laser light, in others the use of magnetic fields or the combination of the two. In this chapter the manipulation of atoms with laser light is described.

2.1 Optical Molasses

The idea of cooling atoms using radiation is based on the principle that radiation has momentum, and from the conservation of momentum, when a particle absorbs radiation its momentum changes. In order to decelerate atoms, lasers are used, as they can provide photons in well-collimated and monochromatic beams [4, 5]. When an atom absorbs a photon coming from the opposite direction to its motion, it loses momentum, while the emitted photons when the atom decays, on average, go in all directions. After the atom has scattered many photons, there is an average deceleration of the atom at the direction of the laser beam. In other words, the atom receives an average force opposite to its movement along the axis of the laser beam, which is called the *scattering force*. This process is illustrated in fig.(2.1).

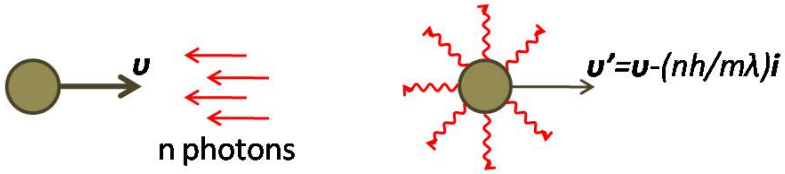

Figure 2.1: The atom absorbs n photons and looses momentum opposite to the direction of the laser beam. v is the initial velocity of the atom, and v' is its velocity after interacting with the photons. m is the mass of the atom, and nh/λ is the momentum transferred to the atom by n photons. i is the vector indicating the direction of the laser beam. The spontaneously emitted photons are emitted in all directions, so on average the total change of momentum due to those photons is zero.

Since we have atoms in a gas that move in all directions, we need a configuration of six laser beams, two counter-propagating beams per axis, that will slow down the atoms under the same principle as before, only this time the atom is decelerated in all directions, therefore its temperature is reduced. This technique is called *optical molasses* [6]. The six beams all come from the same laser, so they have the same frequency. For the atoms that are stationary, the radiation forces balance each other. However for those atoms that are moving, the Doppler effect takes place, and the atoms do not see the same force in all directions. The beams opposing its movement will be seen by the atom as blue shifted and the beams coming from the opposite direction will be seen as red shifted. If the beams have frequency below the atomic resonance frequency, the Doppler shift will bring the beams opposite to the atom's velocity closer to its resonance frequency, and thus the rate of absorption from these beams will be greater. This means that the force opposite to the atom's velocity is greater than that parallel to its velocity, so finally the atom slows down.

2.2 Magneto-Optical Trap (MOT)

The optical molasses technique can be used to cool the atoms, however it is not sufficient to trap them. If now we add a quadrupole magnetic field and choose correctly the polarizations of the beams, we can also have spatial confinement of the atoms, which means we can trap them. This trap is called a *Magneto-Optical Trap* (MOT), and the main idea of the technique is shown in fig.(2.2).

The quadrupole magnetic field is created by two coils with currents in opposite directions. By itself, the magnetic field does not cause the confinement of the atoms. It just causes an imbalance in the scattering forces of the laser beams, and it is the light that finally confines the atoms. In fig.(2.2a) there is a simple example for atoms with a $J = 0$ to $J = 1$ transition. Due to the magnetic field, we have a Zeeman splitting of the three sublevels (with $M_J = 0, \pm 1$) of the $J = 1$ level, which is zero at the point in the middle of the coils ($z = 0$), and increases linearly with distance. The laser frequency is slightly red detuned from the atomic resonance frequency and the polarization of the light is chosen to be circular. If we assume that we have an atom displaced from the center of the trap by a distance $z > 0$, its $\Delta M_J = -1$ transition moves closer to resonance with the laser frequency. Due to the selection rules, the atoms will absorb photons from the σ^- beam, and it will be pushed towards the trap center. For $z < 0$, the $M_J = +1$ state lies below the -1 state, and in that case the atoms absorb photons from the σ^+ beam, and again they are pushed towards the $z = 0$ position. The difference from the optical molasses technique, is that now the force that the atoms receive, is position dependent, and thus the atoms can be trapped.

When there are three pairs of counter-propagating beams perpendicular to each other, we have confinement in all three dimensions, and for that reason the configuration is called a 3D MOT. By removing a set of counterpropagating beams, one can form a so called 2D MOT because confinement is limited to a plane and an atom beam is formed along the axis where light is removed. The physical principles are

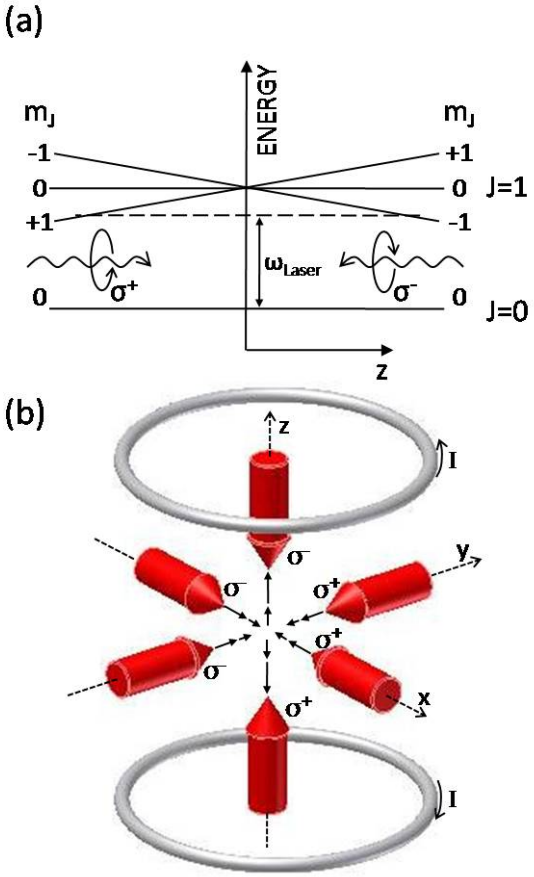

Figure 2.2: Magneto-optical trap (MOT). A combination of laser radiation and magnetic field leads to atoms slowing down and being spatially confined.

the same for the two cases, only that for the 2D MOT there are only four beams used instead of six.

2.3 Re-pumping

The beams used for the optical molasses in our case are slightly detuned with respect to the $F = 2 \rightarrow F' = 3$ transition of the D2 line of ^{87}Rb, so during the cooling process the transition that takes place is between those lines. When we begin with this technique the atoms are distributed in both levels of the ground state ($F = 1$ and $F = 2$ levels). In addition, during the cooling process, there is the probability that some atoms decay from the excited state to the $F = 1$ level (about 1/2000 excited atoms fall into the $F = 1$ state). The atoms in the $F = 1$ level are not able to see the light of the cooling beams as they are very far from resonance with the light frequency (6.8 GHz far from resonance). Since after a number of cycles all the atoms will end up at this state, we will eventually loose all of our atoms. In order to avoid that, we use the *re-pump beam*, which aims to bring the atoms "back in

action" by exciting them back to the $F' = 2$ line so that they can continue with the absorbing - emitting process, until they are cooled down.

2.4 Optical Pumping

In order to further cool our atoms, as required before the BEC can be formed, we need to transfer our atoms to a magnetic trap. However, in order for the atoms to be trapped in a magnetic field, they need to be in a state suitable for trapping by the magnetic field. This means that we have to prepare our atoms in this state before we proceed with the magnetic trapping of the atoms. This is done with the optical pumping beam.

When the atoms are in a magnetic field, they tend to move towards regions with lower or higher magnetic field, depending on their state, so they can be trapped within a region or they can escape. For $m_F > 0$, they move towards low field regions and are characterized as "low-field seekers". On the contrary, for $m_F < 0$, the atoms move towards higher field regions ("high-field seekers") and they cannot be trapped, while for $m_F = 0$, they are not affected by the magnetic field.

The optical pumping beam is in resonance with the $F = 2 \rightarrow F' = 2$ transition, and is circularly polarized, so that only the σ^+ transitions take place. In that way, the atoms tend to go towards the $m_F = +2$ state. Thus after a number of transitions, all the atoms end up in that state, as is shown in fig.(2.3).

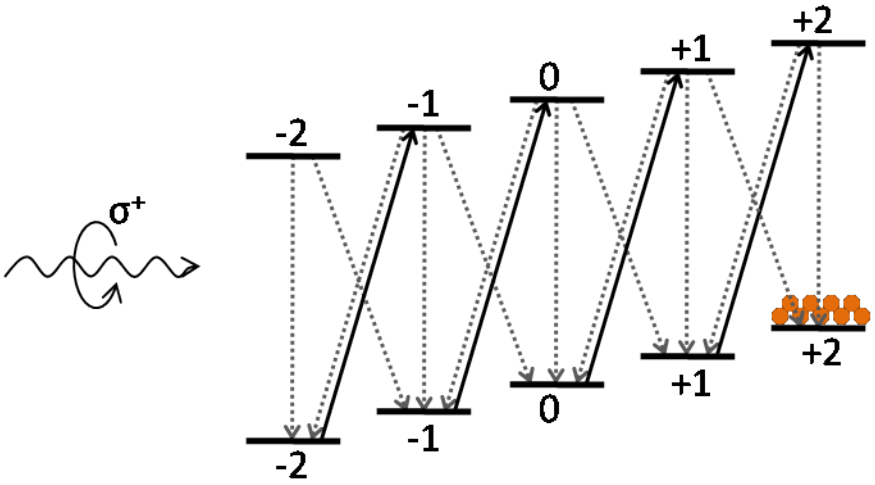

Figure 2.3: Optical Pumping. All the atoms are transferred to the $m_F = +2$ state in order to be trapped by the magnetic field.

2.5 Imaging of the BEC

After creating a BEC, one would like to observe it. For that reason, we must introduce an imaging technique in order to image and then study the atoms contained in

a BEC. For the imaging we use a laser beam on resonance with the $F = 2 \rightarrow F' = 3$ transition of our Rubidium atoms.

The imaging technique is based on the absorption of the imaging beam by the atoms. As the imaging beam is in resonance with the atoms, the atoms absorb some of the light of the beam, and the image that we get is essentially the shadow of the cloud. The image is taken by a high resolution CCD camera. According to this technique, we need to take two photographs, one without the atoms, and one with the atoms, so that we can subtract the one image from the other in order to eliminate the background light. The main idea of the absorption imaging technique is shown in fig.(2.4).

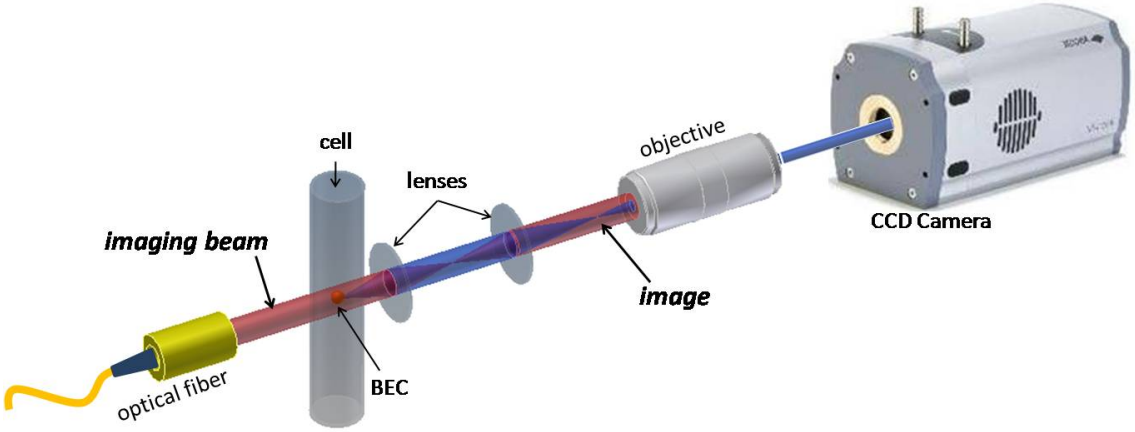

Figure 2.4: Main idea of the imaging technique: the atoms absorb photons from the imaging beam that comes from the optical fiber. The remaining photons that are not absorbed are depicted on a CCD camera and the image of the BEC is essentially its shadow. The imaging beam is in resonance with the $F = 2 \rightarrow F' = 3$ transition of our Rubidium atoms.

Chapter 3

Laser System

In order to do BEC experiments we need lasers very well stabilized and tunable, as we need to slightly change the frequency of the light for the different parts of the experiment, which are the 2D and 3D MOT, the optical pumping and the imaging. In the following diagram (fig.(3.1)) we show the main parts of the laser system:

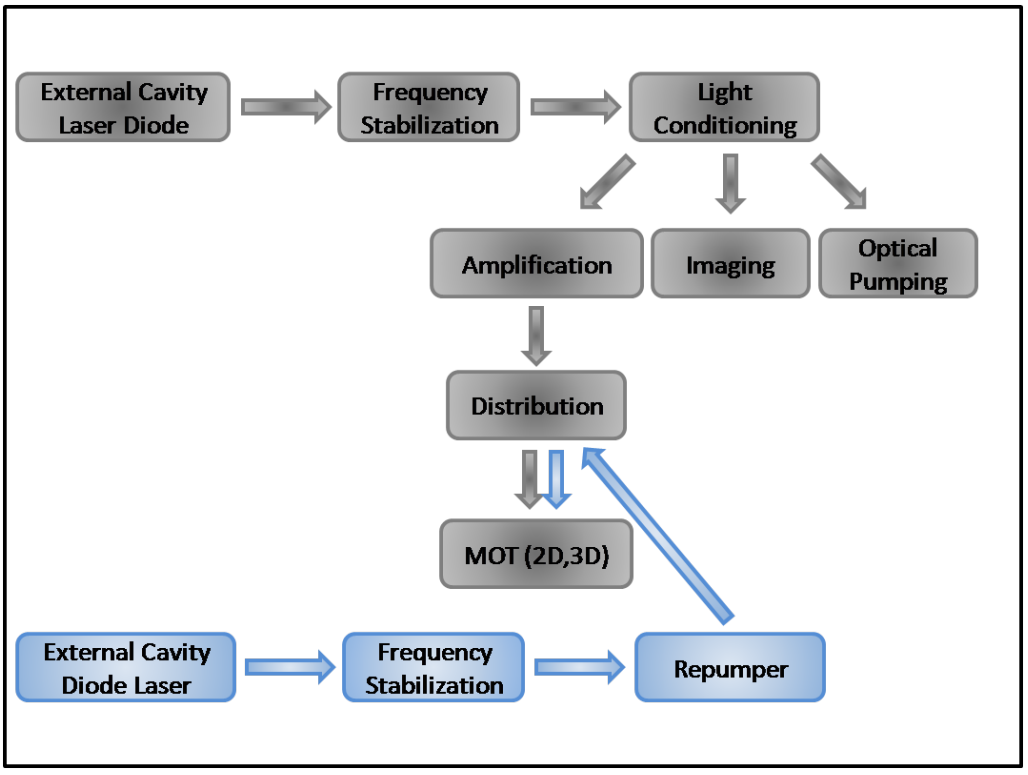

Figure 3.1: General schematic diagram of the laser system: stages from which the light passes in order to be prepared for the several parts of the BEC experiment.

The stages that the light passes before it is ready for the BEC experiment are the frequency stabilization, the light conditioning, the amplification and the distribution. These stages are described in the following paragraphs.

Fig.(3.2) shows the detailed diagram of the laser system, including the frequency and the power that we need for each part.

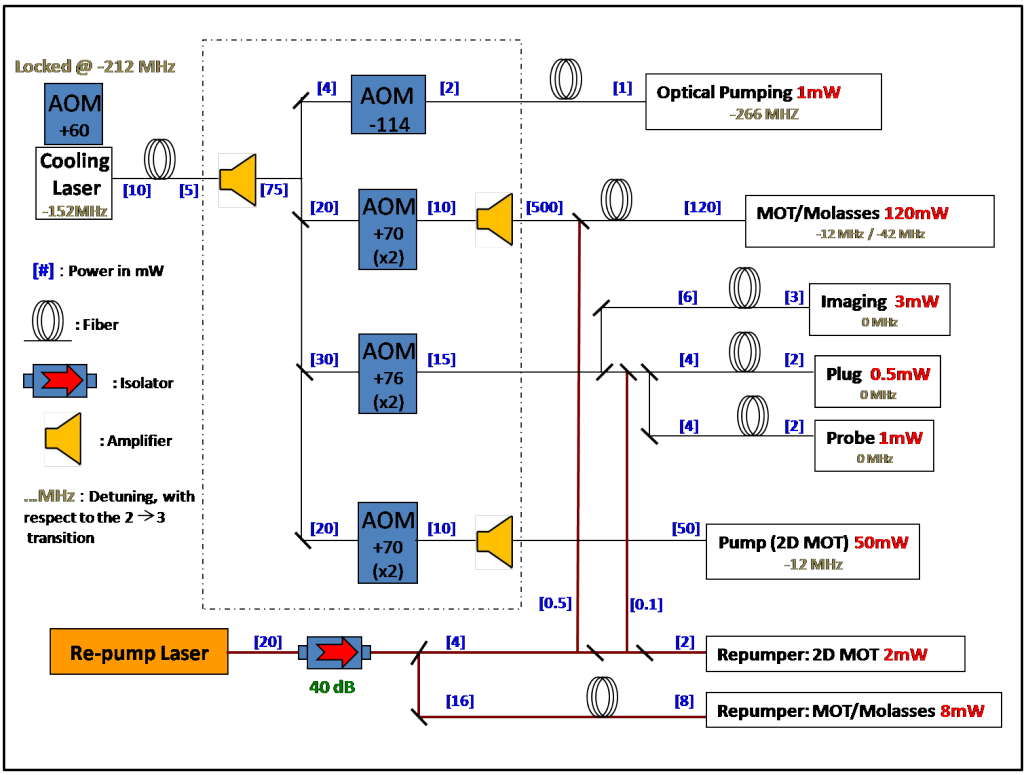

Figure 3.2: Detailed schematic diagram of the laser system.

The frequencies are chosen to drive the required transitions in the ^{87}Rb atoms, used for our experiment. An overall diagram of all the frequencies that we need for the BEC experiments is shown in (fig.(3.3)).

3.1 Frequency Stabilization

For our experiments we need lasers very well stabilized in order to be resonant with certain frequencies. The laser linewidth must be narrow compared to the frequency separation of the $5P_{3/2}$ F=2→3 which means smaller than 267 MHz. To achieve that we use one main laser locked to the F=2→c1/3 crossover resonance of the ^{87}Rb in the case of the trapping laser, and to the F=1→2 line of the ^{87}Rb in the case of the repumper (see fig.(3.3)). The cooling laser is not used directly. It first passes through the Light Conditioning stage (see section 3.2), before it feeds the main parts of the experiment, which are 2D and 3D MOT, the imaging and the optical pumping. The setup for locking the repumper is the similar to that for the trapping laser. Both will be described in more detail in subsection 3.1.2.

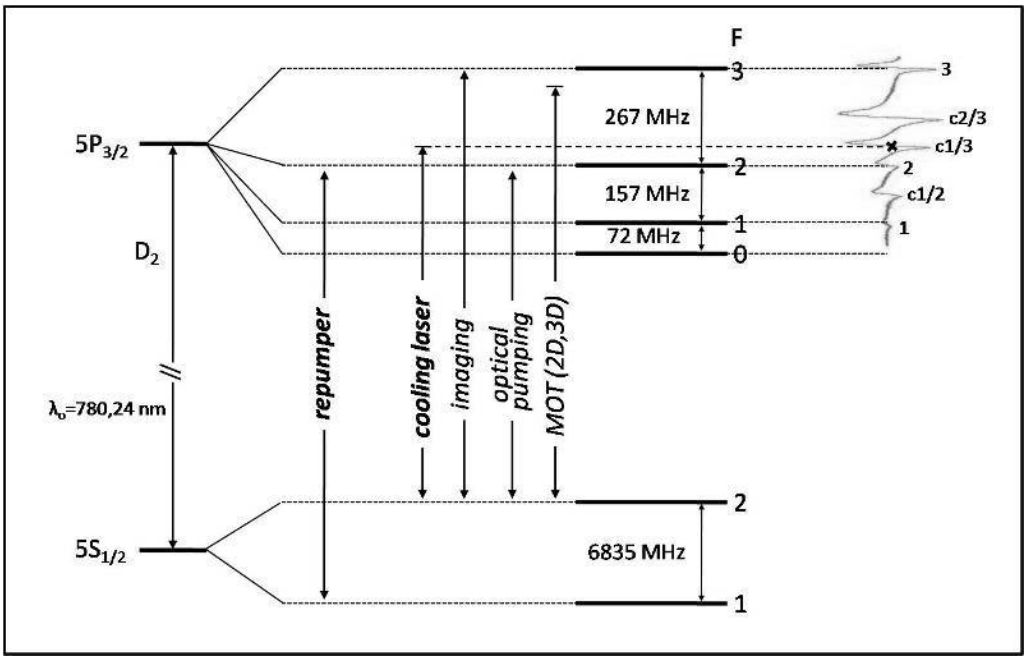

Figure 3.3: Fine and hyperfine structure of the D2 line of ^{87}Rb. The arrows represent the beam frequencies that we use for each step of the experiment (imaging, optical pumping and MOT). In the case of the repump and the cooling lasers, the arrows show the locking frequencies. In addition, the differential signal of the Saturation Absorption Spectroscopy (see subsection 3.1.2) and the locking point for the cooling laser are shown.

3.1.1 External Cavity Diode Laser

The lasers that we use for our experiments are Sharp - laser diodes (120mW 784nm GH078JA2C). The frequency of free running laser diodes is very sensitive to injection current and temperature changes and have large linewidths (∼100 MHz). For this reason, we operate the laser in an external cavity (*External Cavity Laser Diode - ECDL*) [7], which is formed with the help of a diffraction grating, and provides frequency selective optical feedback. The configuration that we use is the Littrow configuration, a diagram of which is shown in fig.(3.4).

In this configuration we use a reflective grating, and depending on the angle we can choose one of the modes of the laser diode. This mode is sent back into the laser and is amplified. The grating is placed on a piezzo, that is used to control its position, and hence the length of the cavity, using external electronic devices. The available power resulting from this setup is approximately 60 mW.

3.1.2 Saturated Absorption Spectroscopy

The next step is the locking procedure, where we chose the desired frequency and make our laser emit only at that frequency. For the cooling laser, the locking frequency is equal to the F=2→c1/3 cross over resonance, while for the repumper it is equal to the F=1→2 resonance of the ^{87}Rb. The following photo (fig.(3.5a)) and

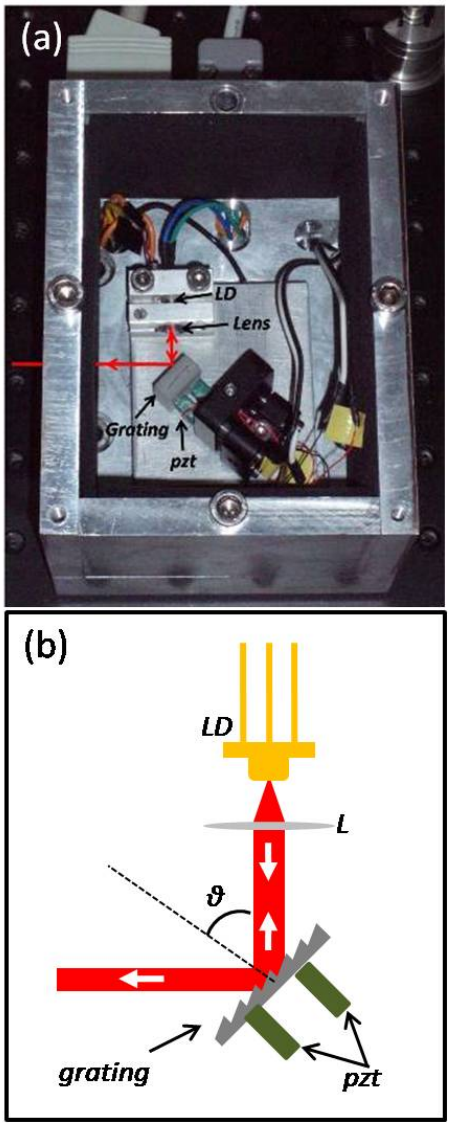

Figure 3.4: The Littrow configuration (a)photo and (b) diagram.

diagram (fig.(3.5b)) show the setup used for the frequency locking.

The whole setup is based on saturated absorption spectroscopy. The light resulting from the ECDL, is separated into two beams, a pump and a probe beam. The two beams travel into a Rb cell in opposite directions. The Rb cell contains two isotopes of Rubidium, ^{85}Rb and ^{87}Rb. In our case, we are interested in the ^{87}Rb transitions, as it is the isotope that we use for our experiments.

If we only used the probe beam the signal measured with a photodetector after the cell would look like the one in fig.(3.6b). The probe beam sees a Doppler broadened transition. It will only interact with atoms for which Doppler shift due to the motion of the atoms compensates the detuning from the atomic transition. This is due to the Doppler broadening of the transitions, because the velocity of the atoms has a Boltzmann distribution. The same happens for the counter-propagating

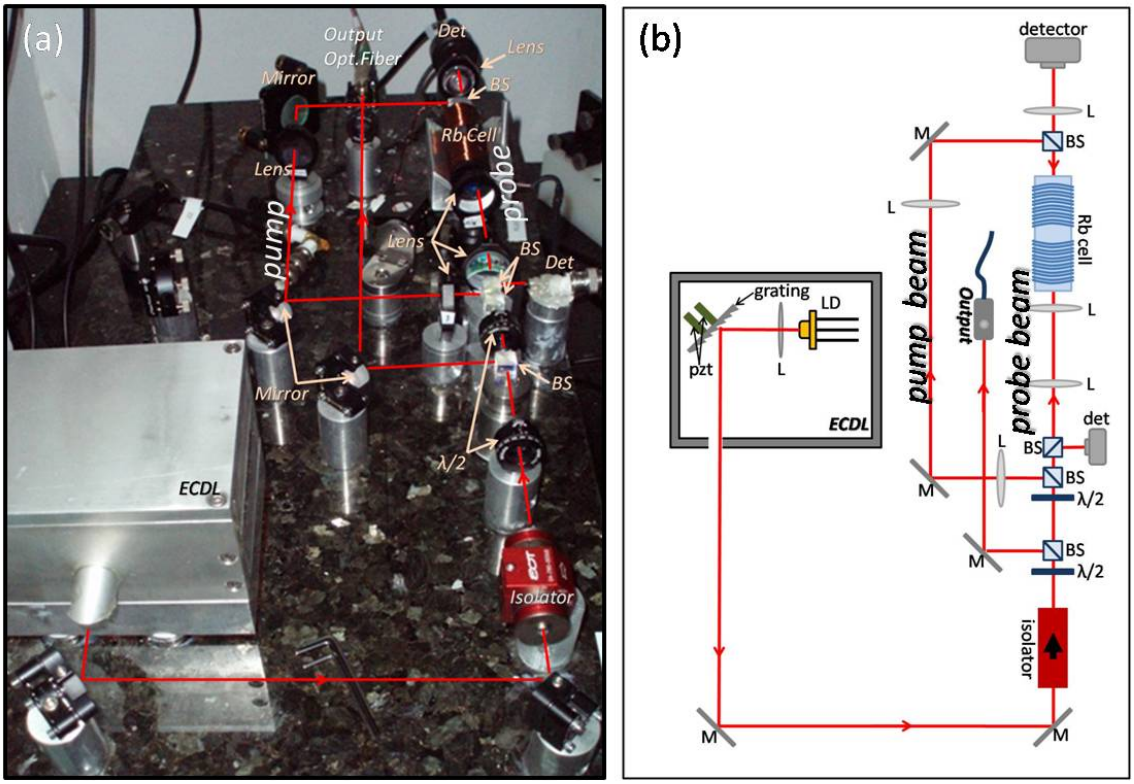

Figure 3.5: Spectroscopy photo (a) and diagram (b). In the diagram, L stands for lens and M stands for mirror. BS are the polarizing beam splitters that are used in order to split the beam into a probe and a pump, and $\lambda/2$ are the half waveplates that are used to control the amount of power that goes to each side of the beam splitters. At the output of the setup, the beam is coupled in an optical fiber.

pump beam, only that the atoms move in the opposite direction.

For both beams to interact with the same velocity group atoms, the laser is tuned exactly must be tuned to the atomic transition. Since they interact both with an identical sample each beam will see less absorption, resulting in small narrow peaks in the broad Doppler absorption spectrum. In fig.(3.7a,b) the absorption signal is shown, while in fig.(3.7c,d) the transitions are shown in more detail. A differential type signal is obtained due to the small frequency modulation.

In order to take advantage of a bigger volume in the cell containing the Rb atoms and thus achieve a larger signal, we need to expand the beams. For that reason we use a set of lenses shown in fig.(3.5). The half waveplates and polarizing beam splitters are used to control the power of the probe and pump beams, as well as the output beam. Finally, the output beam is coupled in an optical fiber, and in the case of the cooling laser it is sent to the light conditioning setup (see section 3.2), while in the case of the repumper, it goes directly to the distribution box (see section 3.4).

The locking procedure demands the use of electronics in order to keep the frequency stable (locked) to a specific value. First, the derivative of the signal is taken,

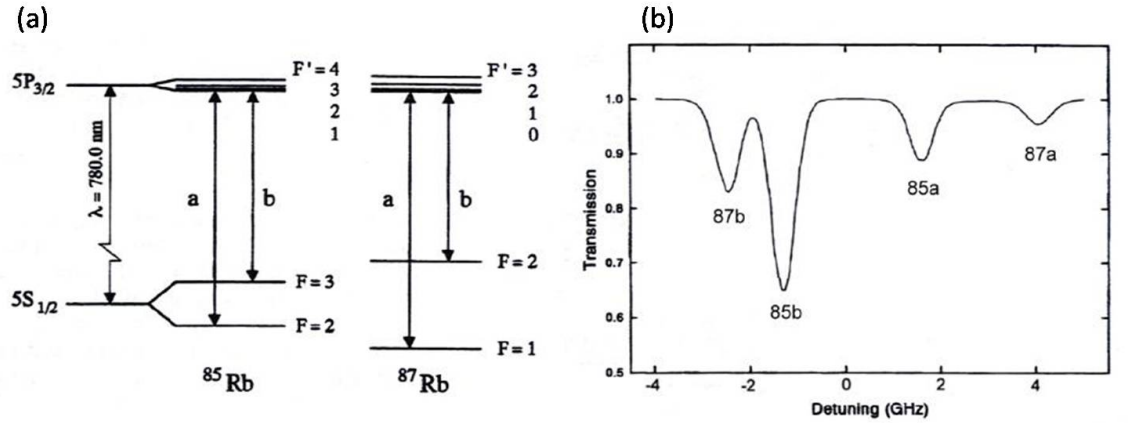

Figure 3.6: Level diagrams for the D2 lines of the rubidium isotopes, ^{85}Rb and ^{87}Rb (a), and the absorption spectrum for those isotopes (b).

enabling the locking electronics to lock to a zero crossing. This greatly reduces systematic errors. After choosing the peak of the spectrum that matches the frequency that the laser must be locked to, we go to the corresponding point of the derivative, which is a zero point, and lock our laser there. When the frequency deviates from that point, adjustments are made to the length of the laser cavity by changing the voltage applied to the piezzos. A general diagram of the electronic control of the laser is shown in fig.(3.8):

In this diagram there are two function generators. The first provides the system with a linear ramp voltage, which is used to ramp the frequency of the laser by changing the voltage of the piezzo, and thus changing the angle of the grating, and the second provides the system with a TTL signal, which goes to the mixer, and a sinusoidal signal, which modulates the injection current of the laser. The first generator is connected to the locking box so that the signal is amplified before going to the piezzo. From the mixer we take the derivative of the signal coming from the detector. The locking box controls the position of the grating in order to keep the frequency in resonance with the selected peak of the Rb. In addition, a low pass (LP) filter is used in order to reduce the noise in the locking signal. Finally, the error signal can be monitored on an oscilloscope.

The difference between the trapping and the repump locking system is the modulation technique that is used. In the case of the repump laser, we modulate the current of the laser, and thus its frequency. In the case of the trapping laser though, we need the frequency to be very stable so we cannot modulate the current of the laser. Therefore, we modulate the states of the atoms using an external magnetic field created by a coil placed around the cell. This solution is more complicated, then that used for the repump laser that we do not really need as much precision, thus we use the simpler solution of the current modulation.

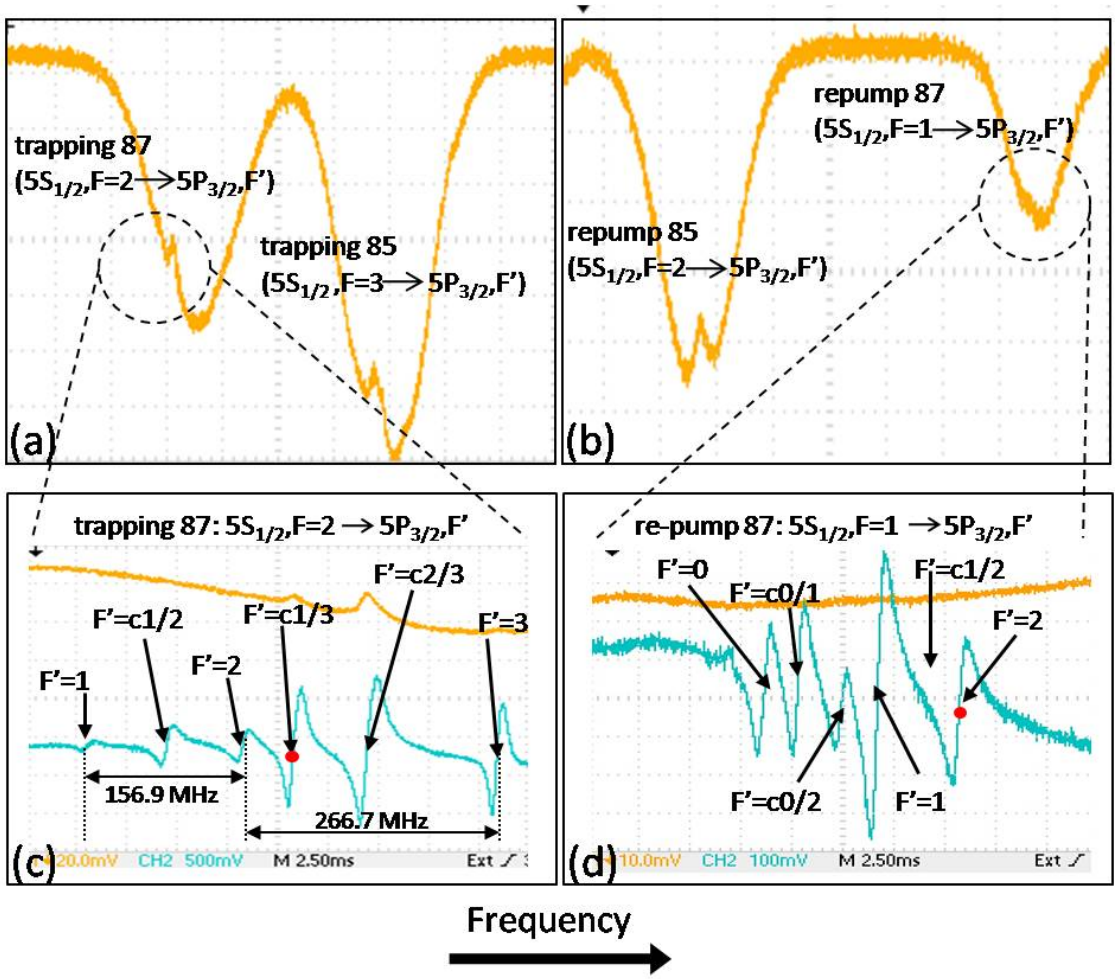

Figure 3.7: (a) and (b): total Rb inverted fluorescence spectrum. (c) and (d): same signal focused on the ^{87}Rb peaks and the corresponding differential signal. The red dots are the locking points for the trapping and the repump laser correspondingly.

3.2 Light Conditioning

In this stage, our beam passes through a series of accousto-optic modulators (AOM), and the result is four beams of four different frequencies which are going to be used for the several parts of the experiment. In fig.(3.9) a diagram and a photo of the setup is shown.

The input light, which is the light coming from the cooling laser, is detuned from the F=2→3 resonance of the ^{87}Rb by -212 MHz. Passing through the first AOM the laser light's frequency changes by +60 MHz. Using an iris, we block all the other orders and we let only the +1 order pass. The polarizing beam splitters are used in order to separate the beams, because from the same beam we have to produce another four. The half waveplates are used to control the amount of power that goes to each beam. The beams must be focused in the AOM, therefore we have placed three lenses before the three first AOMs. After one pass through the AOMs, the

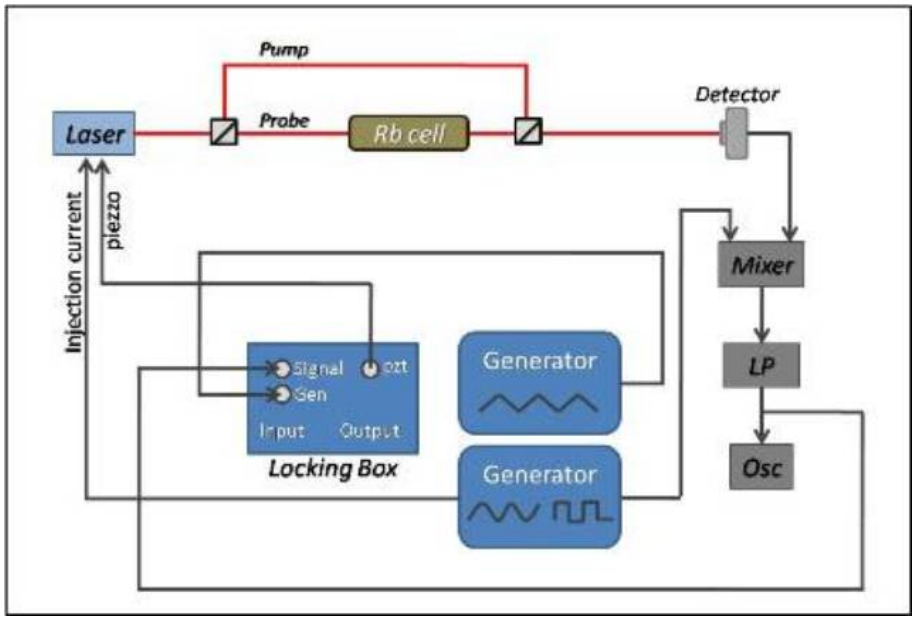

Figure 3.8: Locking electronics diagram.

beams are reflected to spherical mirrors and follow the opposite path passing again through the AOMs. We use spherical mirrors instead of the common flat mirrors, in order that the system becomes completely symmetrical and in that way if the angle of the beam changes, we do not need to realign the system. The angle can be changed if we change the voltage of the AOMs whenever we want to change the modulation. The quarter waveplates are used in order that the beam going back is not reflected by the beam splitter but passes through it. After this path, we take the three beams for the imaging, the 2D MOT and the 3D MOT. The frequencies are 0, -12 and -12 MHz with respect to the F=2→3 line respectively. The fourth beam, which is used for the optical pumping, has a frequency change of -266 MHz applied. For the optical pumping we cannot use the double pass configuration. The modulation which is needed for this case is -115 MHz. For the double pass case, we would need to set the AOM to 57.5 MHz. The AOM that we have can go from 60 to 100 MHz. Therefore this last AOM is used in the single pass configuration. In this case, we have to make corrections in the alignment if we change the voltage of the AOM, which in turn changes the laser beams angle after the AOM. This is achieved by using a set of two wedges. In the end the beams are coupled in optical fibers. We should mention that the power of the beam is reduced each time that it passes through the AOM by 30%. For the double pass case the beam is reduced by almost 50%. The resulting power is 2, 10 and 15 mW for the optical pumping, the 2D and 3D MOT, and the imaging beams respectively.

In fig.(3.3) we show the laser frequencies that we need for each part of the experiment, which correspond to the transitions between the hyperfine levels of the D2 line of the ^{87}Rb. We can see that the repump frequency is far from the others and cannot be achieved using our AOMs, so we have to lock this frequency from the

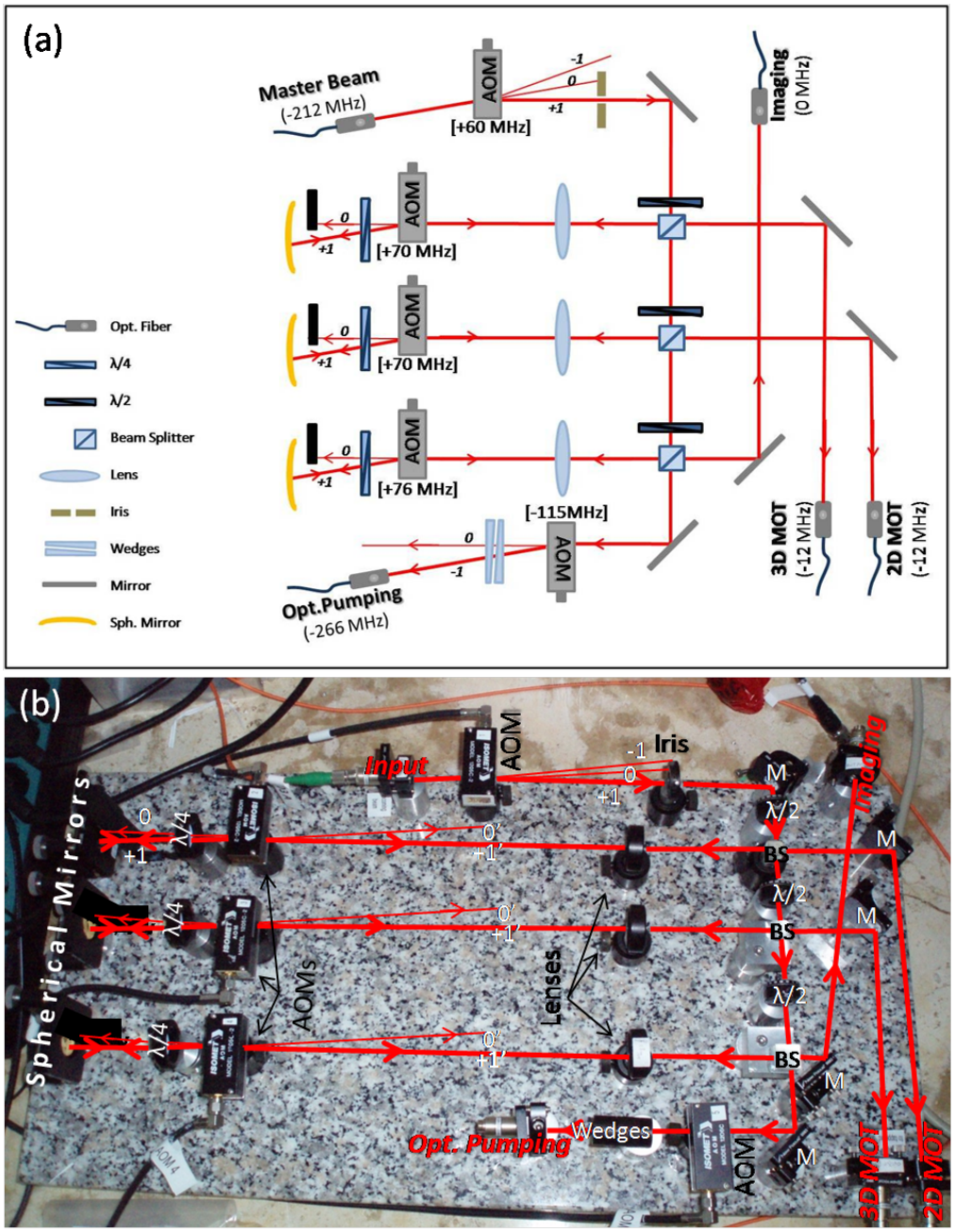

Figure 3.9: In the Light Conditioning stage, the master beam passes through a series of AOMs and modulated in frequency. In (a) there is a diagram of the setup. In brackets there is the frequency of the AOMs, which we set and corresponds to the frequency change of the beam that passes through. In parenthesis there is the detuning of the beams with respect to the 2→3 line of the ^{87}Rb. In (b) there is a photograph of the actual setup.

beginning. The others (imaging, optical pumping and 2D-3D MOT), all result from the same laser (the cooling laser) after passing from the light conditioning stage.

3.3 Amplification

After the stage of modulation, and after all the losses that the beam has experienced until that part (losses from the AOM: approximately 30% after each pass), the power of the light that has remained in the 3D MOT beam is of the order of 10 mW. However, for the MOT we need at least 150mW, which makes it necessary to amplify the light. This is done with the help of a Tapered Amplifier, which is a laser diode based on GaAs semiconductor, with a taper shaped gain region. After the amplification stage, the power of our beam can be up to 1000 mW. The subject of amplification will be discussed explicitly in Chapter 5.

3.4 Distribution Box

Finally, before the light is sent to the experiment, the beam needs to be separated and distributed, especially for the case of the 3D and the 2D MOT. This happens in the distribution box. A schematic diagram and a photograph of the distribution setup for the 3D MOT is shown in fig.3.10.

The beam passes through a series of polarizing beam spitters, and is divided into six beams of equal power. With the aid of waveplates we control the amount of light that goes to each beam. Finally, the resulting beams are coupled into optical fibers in order to be directed to the experiment. The power of each one of the output beams depends on the input power. The coupling efficiency that we have is approximately 70%. That means that the remaining power for each one of the resulting beams is almost the 11,5% of the initial beam.

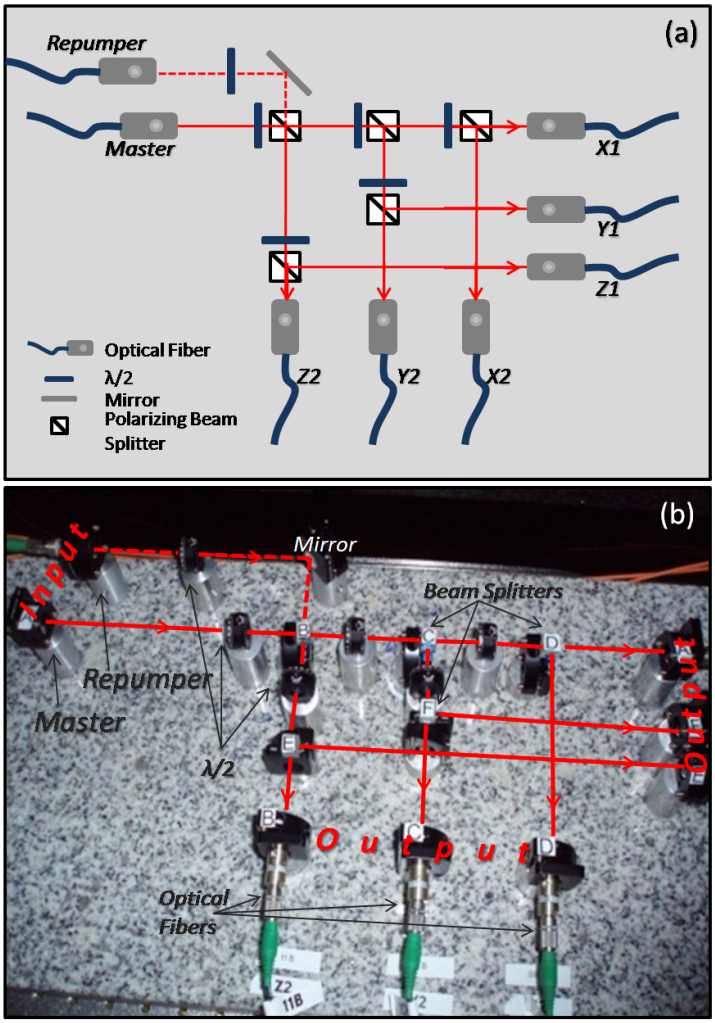

Figure 3.10: (a) Diagram and (b) photograph of the distribution setup. The master beam is splitted into six beams of the same power which will be used for the 3D MOT.

Chapter 4

Amplification

For the amplification of our master laser, we use a Tapered Amplifier (TA) device from EagleYard photonics. The TA is very similar to a common laser diode, with the difference that its surfaces are coated with an antireflection layer, in order that there is no cavity formed by the gain region. In that sense the amplifier is not a laser. In addition the gain region has a tapered shape (see fig.(4.1). The beam that enters the device is expanded, and in that way the device can support much higher power, without damaging the output surface, while the beam remains diffraction limited [8, 9].

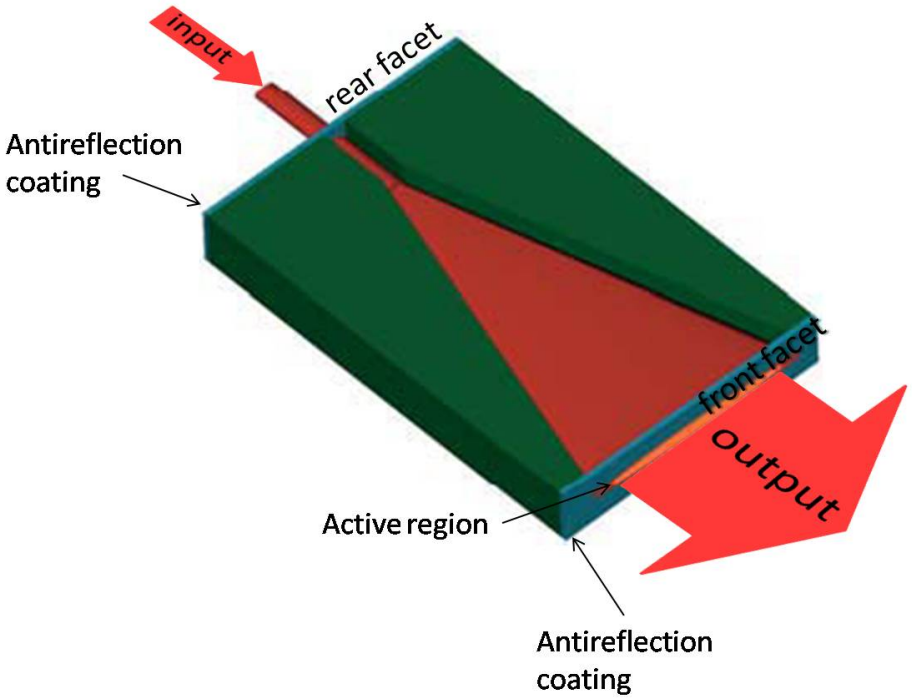

Figure 4.1: Tapered Amplifier gain region.

The characteristics of the device are shown in the table of fig.4.2.

Parameter	Symbol	Unit	min	typ	max
Operational Temperature at case	T_{case}	°C	0		40
Forward Current	I_F	A			2,5
Center Wavelngth	λ_c	nm	770	780	785
Gain Width (FWHM)	$\Delta\lambda$	nm	10	20	
Temp. Coeff. of Wavelength	TC_λ	nm/K		0,25	
Output Power	P_{out}	mW		1000	
Amplification		dB		13	
Saturation Power	P_{sat}	mW		50	
Operational Current	I_{op}	A		2,5	
Cavity Length	l_c	µm		2750	
Input Aperture (at rear side)		µm		3	
Output Aperture (at front side)		µm		190	
Divergence parallel (FWHM)	$\Theta_{\parallel}$	°	7	10	13
Divergence perpendicular ($1/e^2$)	$\Theta_{\perp}$	°		28	
Astigmatism		µm	325	375	425
Polarization				TM	

Figure 4.2: Characteristics of the Tapered Amplifier device at ambient temperature $T_{amb} = 25^oC$.

The gain width of the TA is approximately 20 nm with a central wavelength at 780 nm. The TA device amplifies the input beam 20 times, giving up to 1 Watt of output power. Since there is danger of breaking the rear surface of the chip, it is recommended that the injection beam does not exceed the $50mW$. The geometry of the active region of the TA leads to an ellipsoid, astigmatic beam which requires correction with the use of lenses.

4.1 Implementation

In order to perform BEC experiments, because of the complexity of the setup, we need every single part of the experiment to be extremely stable and reliable. Especially for the case of the amplification part, where the dimensions of the chip make the alignment very sensitive to thermal drifts. Thus we need to pay attention on the design and construction of the TA mount. The mount design is described below.

4.1.1 Mounting

The base of the TA is made of copper which has better thermal conductivity than aluminum, so that we can achieve more effective cooling of the device. The temperature stabilization of the device is achieved with the help of a peltier element

controlled by a Thorlabs TED350 Temperature Controller. The sensor that we use is a $10k\Omega$ thermistor. Due to the dimensions of the active region of the TA, which are of the order of $5\mu m$, an expansion of the base of that order destroys completely the alignment. In order to avoid that we have placed and glued the lenses needed for the focusing of the injecting beam, and the collimation of the resulting beam on the same base. In that way, the lenses follow the expansion of the base and the sensitivity of the system due to thermal drifts is now defined by the size of the beam, which means of the order of $2mm$. A drawing the TA base is shown in fig.4.3.

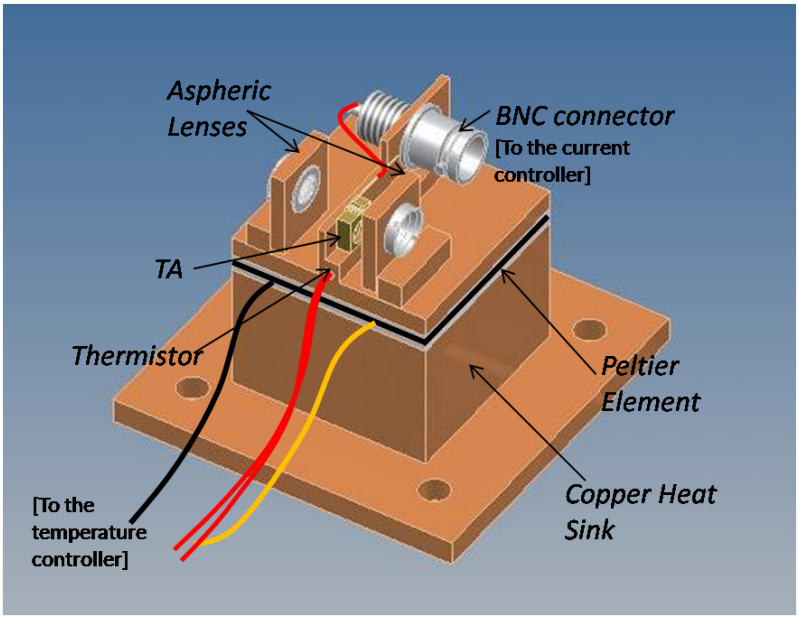

Figure 4.3: TA base. It is made of copper for better thermal conductivity, and uses a peltier element as a cooling device. The lenses are placed and glued on the base for better stability of the system.

The aspheric lenses that we use here are both the same, GelTech f=4.5mm, bought from ThorLabs (C230TM-B). In order to collimate the outcoming beam, only the aspheric lenses that we use are not sufficient. Due to the rectangular geometry of the device, the beam exits the TA with different expansion angles for the two axis. In order to correct this astigmatism and elliptic beam shape, we placed a second lens, a ThorLabs LJ1821L1-B cylindrical lens with focal length $50mm$, and dimensions $20 \times 22mm$, to collimate the horizontal axis, as the vertical axis is already collimated by the aspheric lens.

Any light reflected back into the TA will be amplified and re-emitted, thus forming a cavity. If the intensity of the back-reflected light is too large it can destroy the TA chip. In order to avoid this we use an isolator. The controller that we use in order to provide the TA with current is a Thorlabs LDC340 Laser Diode Controller.

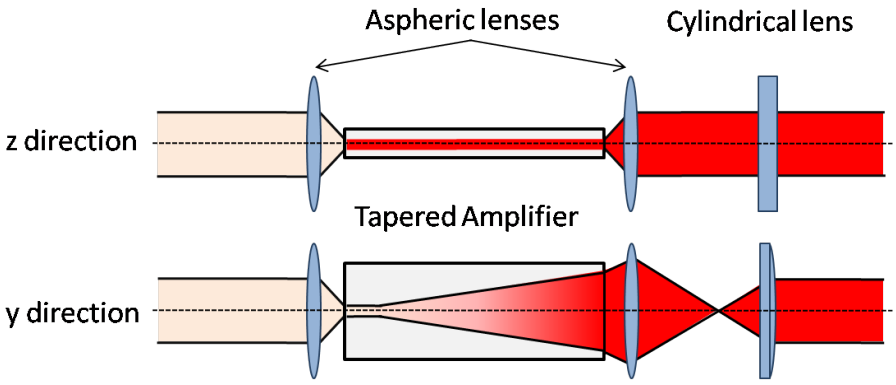

Figure 4.4: Lens system for the correction of the astigmatism of the outcoming beam.

4.1.2 Single Pass Configuration

The common setup [10] in order to have light amplification is shown in fig.4.5:

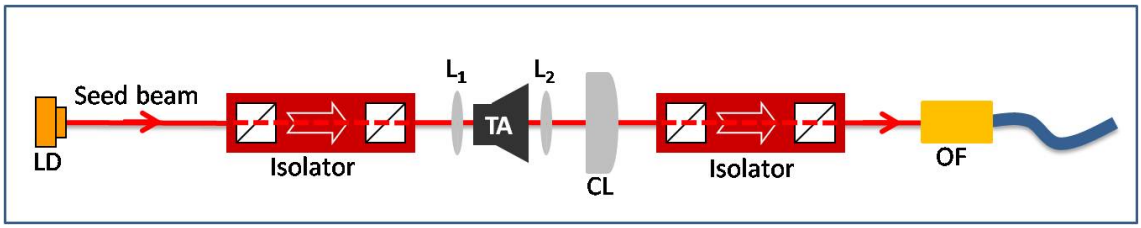

Figure 4.5: Single Pass configuration. *TA* is the Tapered Amplifier device, M_1 and M_2 are mirrors, L_1 and L_2 are the aspheric lenses used for correcting the TA beam, *CL* is the additional cylindrical lens used for collimating the beam at the horizonal plane, and *OF* is the single mode optical fiber used in the end to drive the beam. The seed beam enters the TA from the rear side and is being amplified.

This kind of configuration is called single pass, as the light passes through the active region only once. The seed power must be from 30 to 50 mW. Since the available power is much lower (less than 10 mW), the use of an additional diode laser as a pre-amplifier is required. This laser diode is a Sharp laser diode (GH078JA2C) that can give power up to 120mW and emits at 784nm. As this type of lasers has a multimode cavity, it can easily support the mode of the master laser and be locked to its frequency. This additional diode is called slave laser, as it "follows" the master laser. In that way we achieve the required power to be seeded in the TA. The diagram of the setup including the slave laser is shown in fig.(4.6).

The output beam from the TA is coupled in an optical fiber for the reason that the system becomes more flexible and the background coming from the amplified spontaneous emission of the TA is eliminated, as it cannot be guided by the fiber effectively.

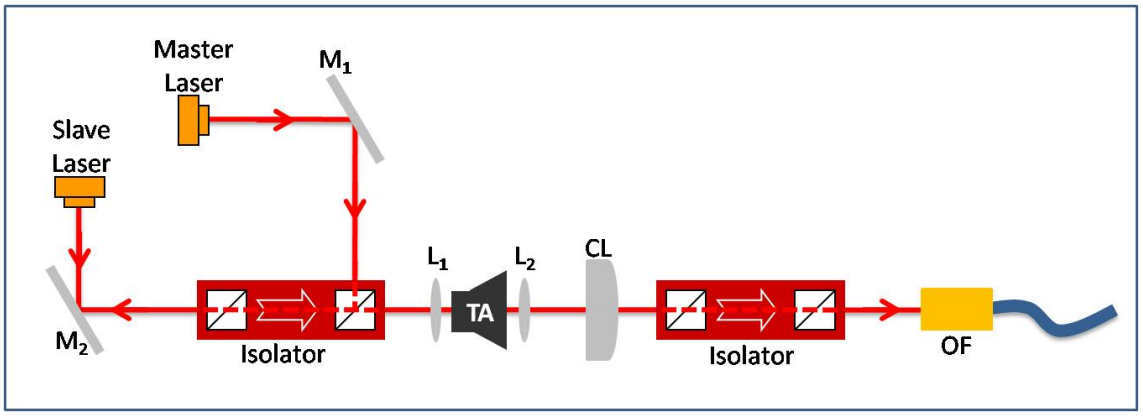

Figure 4.6: Single Pass configuration including a slave laser diode as a pre-amplifier. In order to seed the slave laser we use the beam splitters of the isolator, as is shown in the diagram.

4.1.3 Double Pass Configuration

In order to achieve maximum output power using minimum injection power at minimal complexity, and because we want to avoid the use of the slave laser, we tried a slightly different configuration, where the light to be amplified passes through the TA twice, so it is amplified two times. In such a way, we need much less injection light, while the setup becomes simpler and easier to align. The light enters the TA from the front side, and, after it exits the rear side, it is back reflected by a mirror, placed perpendicular to the surface of the TA, and enters the TA again. As the system is (almost) symmetrical, the light reflected by the mirror has the right size and shape that matches the shape of the TA active region, and thus guarantees maximum coupling efficiency.

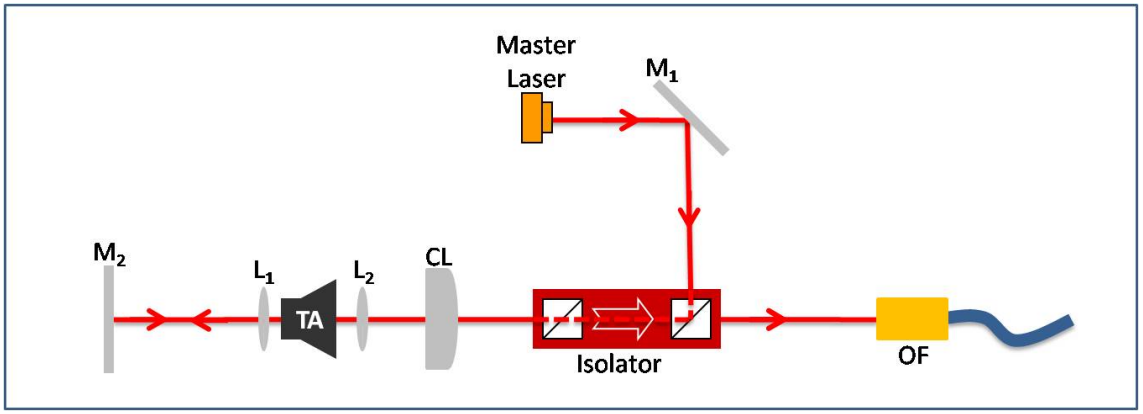

Figure 4.7: Double Pass configuration. The setup is very similar to the Single Pass, only that this time the beam travels through the TA twice, and there is no need for a slave laser diode.

The advantage of this configuration is that we achieve the same output power as with the single pass, however, use far less injection light. Thus this configuration

is extremely efficient in comparison with the normal single pass method. Using this configuration we can have injection power of the order of *0.5 mW*, and with that input the output power can be more than *600 mW*. For the single pass, in order to have the same results, we need injection power approximately *50 mW*, which means 100 times more power. In addition, we need less components for the double pass setup, as we avoid the use of the slave laser with its controllers, and the second isolator, and thus the system becomes simpler and cheaper.

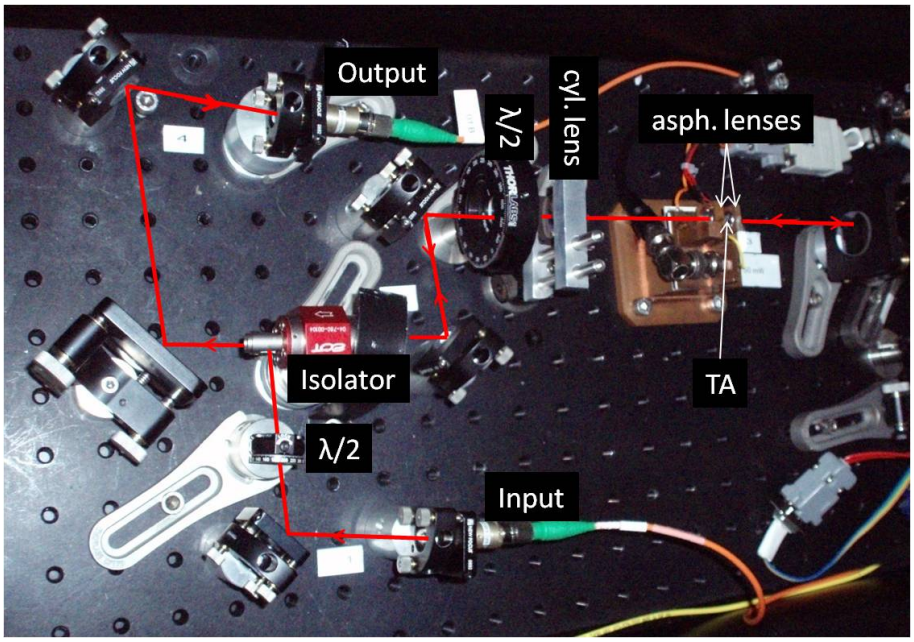

Figure 4.8: Double Pass configuration. The setup is very similar to the Single Pass, only that this time the beam travels through the TA twice, and there is no need for a slave laser diode.

4.2 Characterization of the System

4.2.1 Unseeded Operation

The operation principles of the TA are similar to those of every other laser diodes. Therefore, even when there is no injection light, the TA emits in the presence of an injection current, I_{TA}. In the absence of feedback the unseeded output is dominated by amplified spontaneous emission over the whole bandwidth of the gain. The emission in this case is not a narrow width line as in lasers, and cannot be used, however by studying it we can make many conclusions about the device.

In the following paragraphs we analyze how the TA unseeded operation is affected by changes in the temperature or the injection current. By changing the temperature we can see how the output power and the central wavelength is modified. While if we change the injection current and measure the output power, we can define the

lasing threshold for different conditions of operation. This will help us to define under which conditions we have the best performance of the device.

Temperature Dependence of the Central Wavelength and the Power In the case of the unseeded operation, the spectrum of the resulting radiation is a broad one (FWHM $\approx$ 25 nm). In figures 4.9 we see how the several spectra look like for different temperatures and different injection currents. The central wavelength

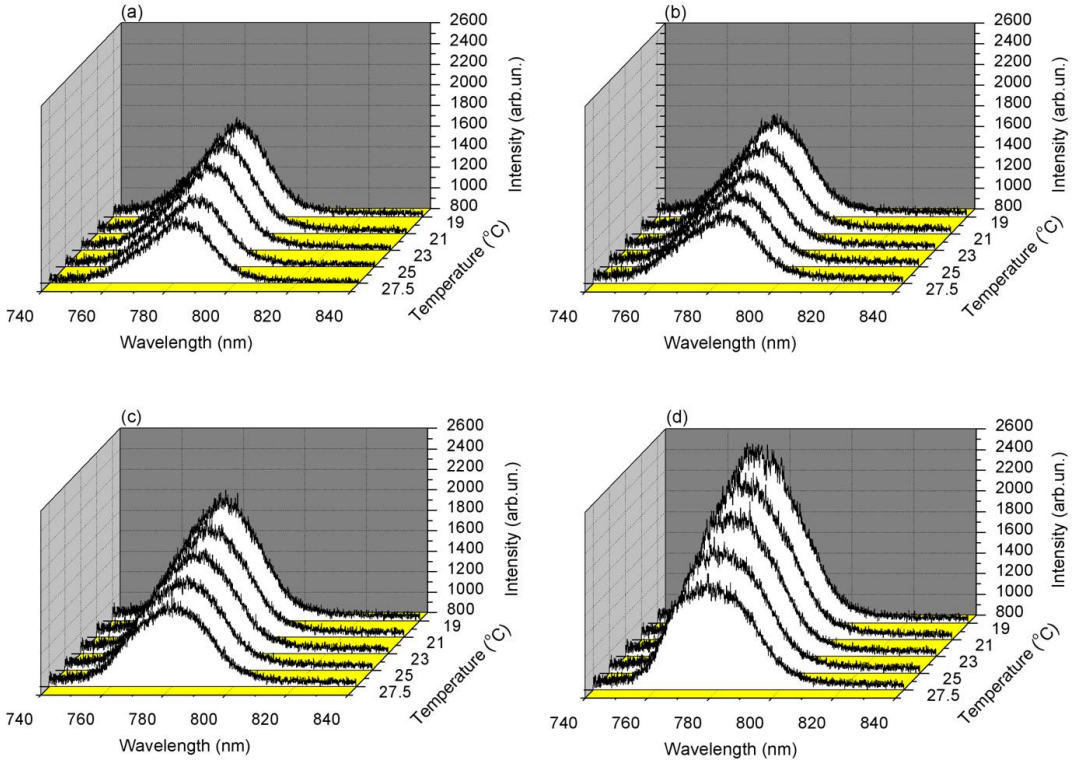

Figure 4.9: Spectra of the Amplified Stimulated Emission for the unseeded operation of the TA for different injection currents: (a)I=1,5 A, (b)I=1,757 A, (c)I=1,997 A and (d)I=2,25 A.

changes as we change the temperature and the injection current. The same also happens for the power. Increasing the current, or decreasing the temperature, the power increases dramatically.

In order to see more closely how the central wavelength behaves, we made a plot of the central wavelength of the amplified stimulated emission of the device for different temperatures and different currents. We observe that the central wavelength changes for both cases. In fig.4.10 we see that the wavelength increases as we increase the temperature, however decreases as we increase the current. Given that our master laser emits at a wavelength of 780 nm, we have to choose our conditions of operation which give a central wavelength as close as possible to the master laser

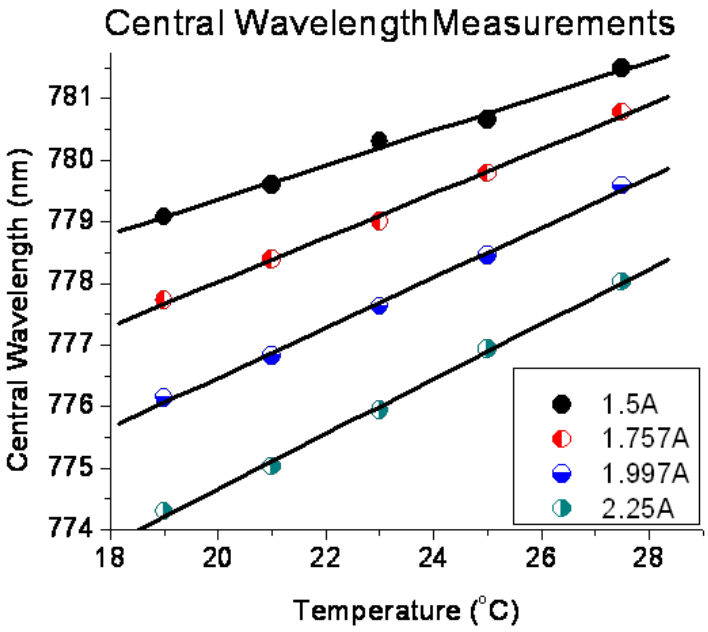

Figure 4.10: Central wavelength of the amplified stimulated emission for the TA unseeded operation, as a function of the temperature, for different currents. We observe how the wavelength increases for smaller current and higher temperature.

wavelength. That means that the temperature shouldn't be too low and the current should not be too high. According to fig.4.10, the best combination occurs at a temperature around 23 ^{o}C and a current around 1,5 A. However that means that we have to compromise on the power.

This can be seen in fig.4.11. As the temperature decreases, the output power of the TA increases rapidly. This fact adds another constraint for the choice of the operation conditions of the TA.

Taking the corresponding measurements for the small side, we find the same results. In the figures that follow are shown the spectra of the amplified stimulated emission taken at the small side of the TA for two values of injection current (fig.(4.12)), the center wavelength as a function of the temperature (fig.(4.13)) and the output power again as a function of the temperature (fig.(4.14)).

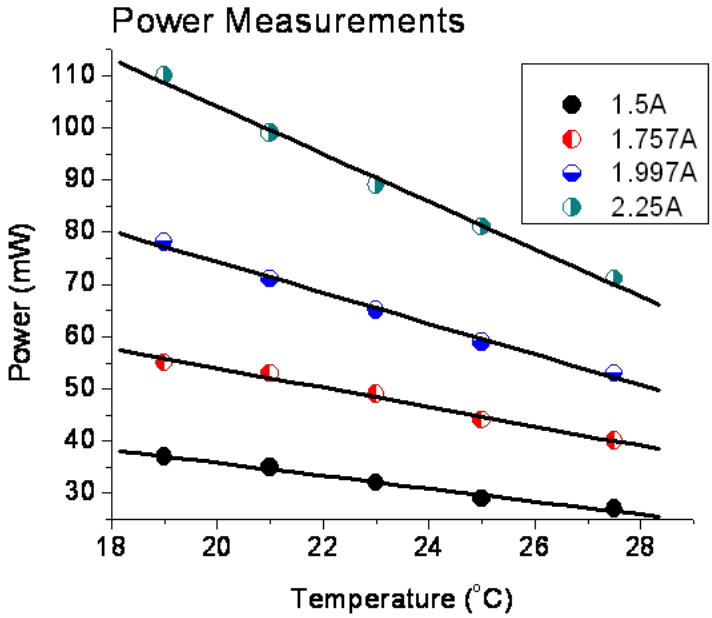

Figure 4.11: Power of the amplified stimulated emission for the TA unseeded operation, as a function of the temperature, for different currents. For lower temperatures we have higher power.

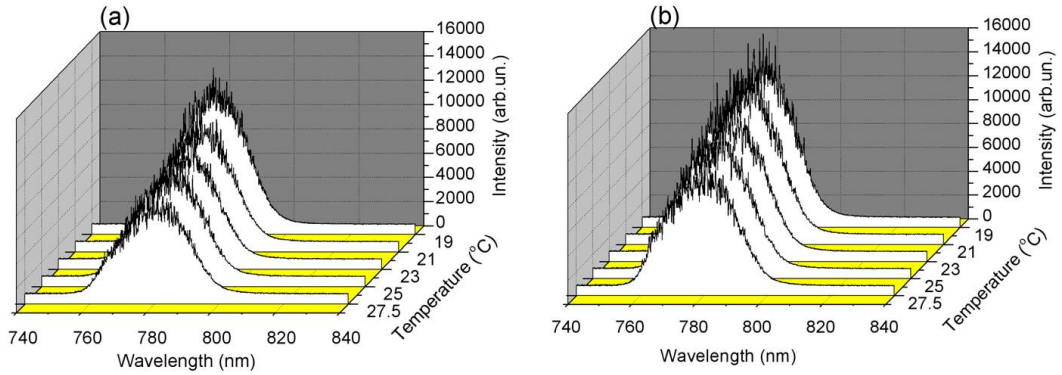

Figure 4.12: Spectra of the Amplified Stimulated Emission for the unseeded operation at the small side of the TA for different injection currents: (a)I=2,058 A and (b)I=2,256 A.

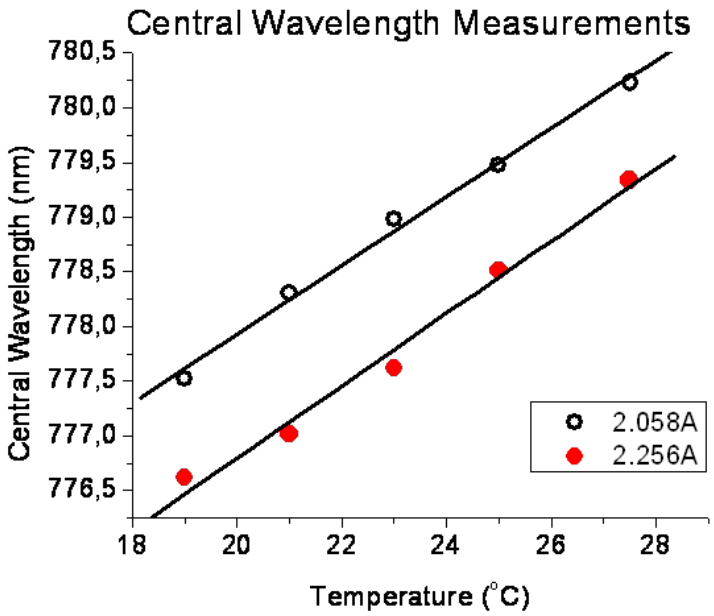

Figure 4.13: Central wavelength for the TA unseeded operation at the small side of the device, as a function of the temperature.

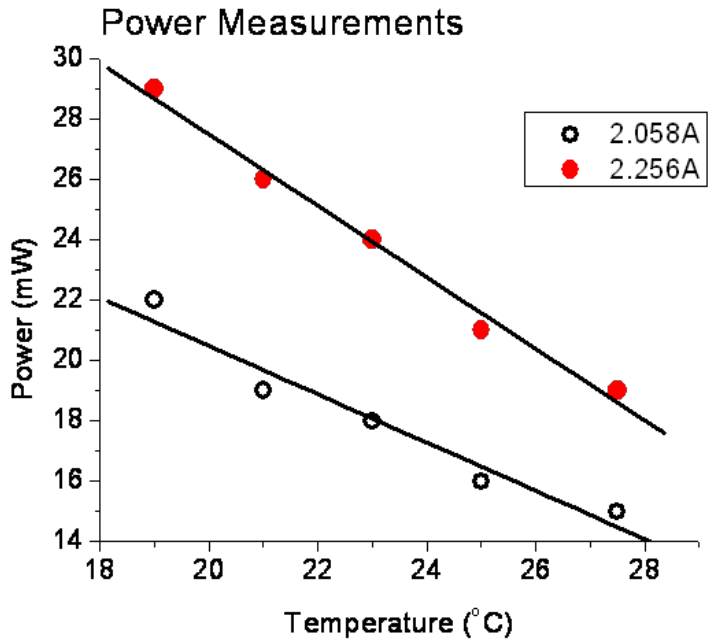

Figure 4.14: Power of the amplified stimulated emission for the TA unseeded operation at the small side of the device, as a function of the temperature, for two different currents.

Injection Current Dependence of the Power By making a graph of the output power as a function of the injection current, we can find the threshold current of the device. This is the point where the graph starts to be linear. More specifically, in our case this happens for I_{inj}=I_{thres}=1,6 A. The graph is shown in the following figure:

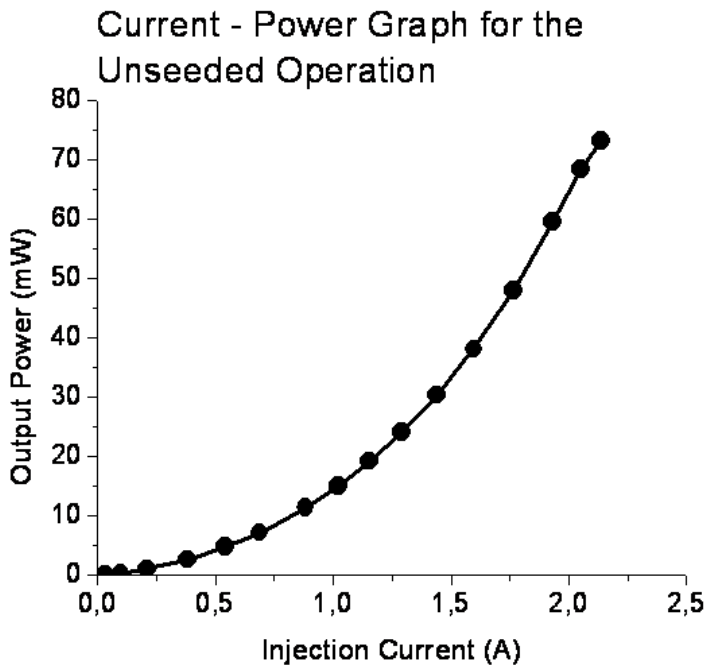

Figure 4.15: Power of the amplified stimulated emission for the TA unseeded operation as a function of the injection current.

4.2.2 Amplification of the Seeded Light

After defining the best temperature and current conditions we are ready to inject our master laser in the TA in order to amplify it. In the following paragraphs we study the properties of the resulting light. We describe the measurements that we made concerning the power, the spectrum and the profile of the output beam as a function of the power of the seeded beam (P_{seed}). All the measurements that follow use the double pass configuration at a constant temperature of $T_{act} = 10.47k\Omega = 24^oC$.

Threshold Current We made measurements of the threshold current of the TA for different injection power, and saw that the threshold current decreases as we increase the power of seeded beam. In fig.(4.16) we show these results:

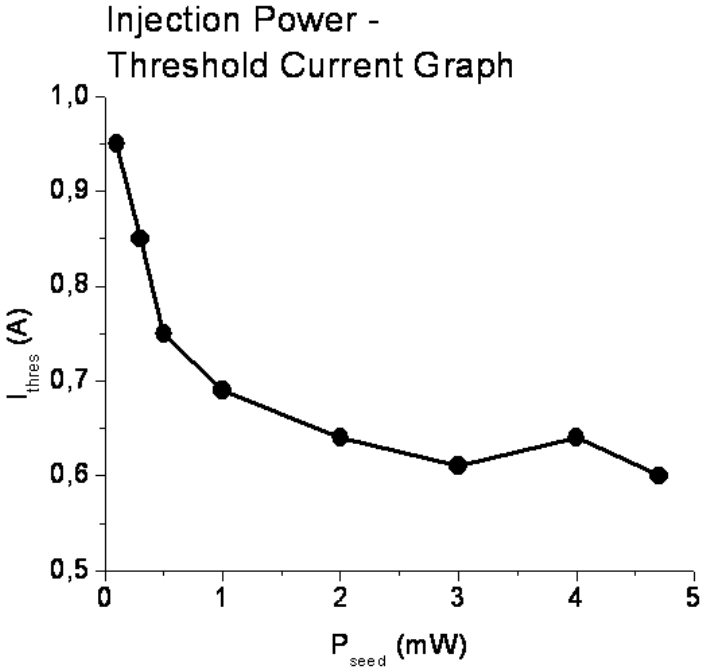

Figure 4.16: The threshold current of the TA as a function of the P_{seed}. The threshold current decreases for greater values of the injection power.

Power In this paragraph we describe the behavior of the TA as we change the power of the injection light. In fig.4.17 we can see the maximum power and the maximum current for different P_{seed}. As higher seeding power leads to a higher output power we need to decrease the injection current in order to keep the power at the rear side of the TA below $50mW$, otherwise there is danger of breaking the surface of the chip. This fact limits the maximum current that we can inject in the TA, and hence the output power. This behavior is shown in fig.(4.17). The values

of the current and the output power are such that for any value of the P_{seed} we have 50 mW at the rear side.

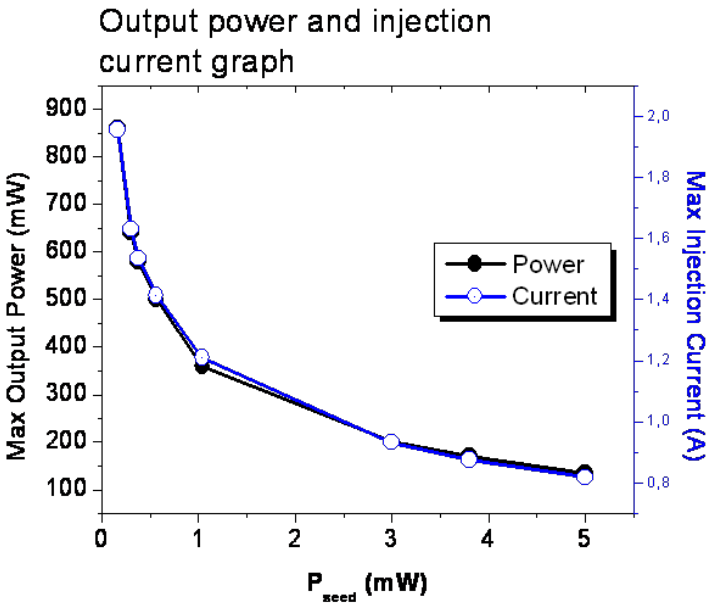

Figure 4.17: Maximum output power and maximum injection current for different seed power. For all the values the power at the small side of the TA is kept constant and equal to 50 mW.

The values of the P_{seed} range from 0,1 to 5 mW. As we can see, for smaller P_{seed} we have greater values of P_{out}. This is normal, as for smaller P_{seed} we can have higher injection current. Smaller P_{seed} is obviously more convenient for us and with a first sight things seem to be very optimistic. However, we have to check the spectrum of the output beam, to see if all this power is contained in the amplified light or in the background of the TA. In other words, we have to check whether the injection beam is enough to suppress the spontaneous emission of the TA.

Spectrum As shown before, the spectrum of the light coming out of the TA, when there is no injection, is a broad spectrum that looks like a Gaussian, and comes from the spontaneous emission of the electrons and holes as they are being recombined. When we inject light, this radiation is suppressed by the stimulated emission and thus, in the spectrum, this background is reduced, while a peak appears in the spectral position of the injection beam. A spectrum like this can be seen in fig.4.18. We can see how the background drops and how the peak occurs at exactly 780 nm which is the wavelength of our master beam. In some cases this spontaneous background can be problematic. Our purpose is to reduce as much as possible the background and increase as much as possible the peak. We define a measure of the quality of our beam as the peak-to-total ratio. This ratio results by the integration of the total spectra and the peaks separately. In our case we need the maximum peak-to-total ratio.

In fig.4.19 we can see the peak-to-total ratio for different P_{seed}. The error bars come from the statistical error, as we have taken many measurements for the same P_{seed}. According to the graph, the ratio seems to be low for lower P_{seed}, and increases for increasing the P_{seed}. For seed powers below $0.5mW$ the peak-to-total ratio is relatively low ($< 80\%$). Above $0.5mW$ however, 93% of the light is emitted at the frequency of the seeding laser. If we remember the results from the previous paragraph, we have to keep our injection power as low as possible, in order to have the maximum output power.

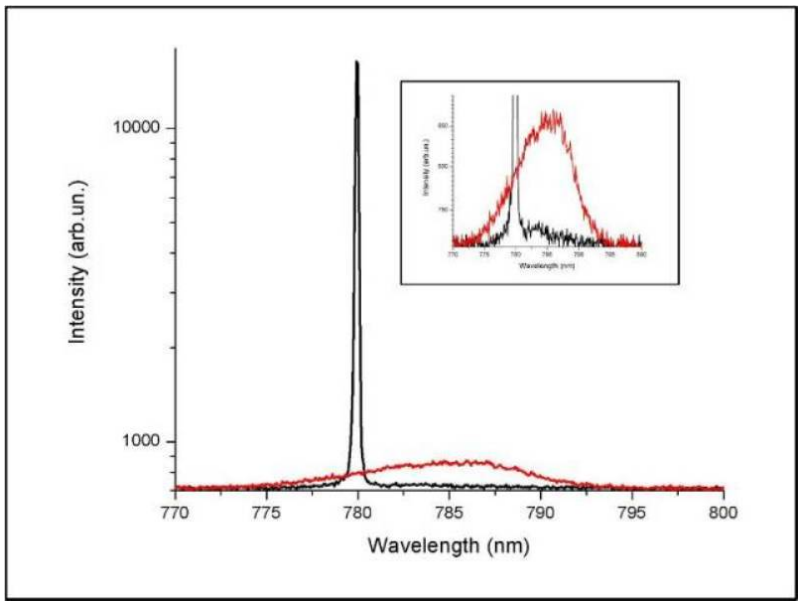

Figure 4.18: Spectrum of the output beam of the TA for P_{seed}=0.8 mW. In the inset there is a magnification of the spectrum, so that the background can be visible. The vertical scale is in a logarithmic scale. The suppression of the spontaneous emission is obvious.

Beam Profile As we mentioned in paragraph 5.1.1, we use a set of lenses in order to collimate the beam coming out of the TA. The beam that results has a similar

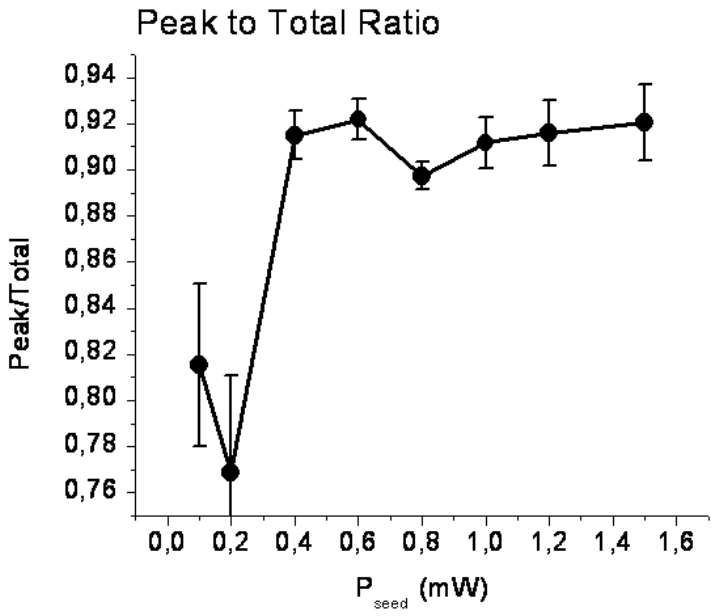

Figure 4.19: Ratio between the power contained in the peak of the spectrum (amplified light) and the total power (amplified light plus spontaneous emission).

profile to the profile shown in fig.(4.20).

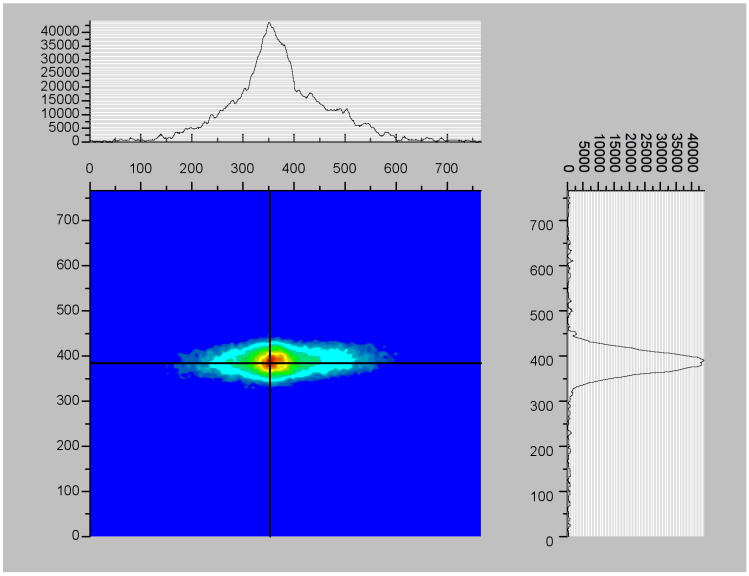

Figure 4.20: Profile of the beam after the TA.

We can distinguish the amplified beam (central bright spot) from the surrounding background, coming from the Amplified Stimulated Emission of the TA. The

background is not collimated by the lens system. This fact is in our favor, as later it can be separated from the useful, central beam, using the optical fiber. The background, due to its shape and divergence, cannot be coupled effectively in the fiber and is lost. In that way spectral filtering is achieved, as we will see in Section 4.3.

4.3 Beam quality after the Optical Fiber

As mentioned before, the output light is driven in a single mode optical fiber. This adds intensity losses to the system, as the beam that exits the TA is not perfectly circular, so we do not have a high coupling efficiency (about 50%). However the advantage of the use of an optical fiber is that it isolates the system from the other parts of the experiment, in the sense that it decouples the optical alignment of the individual subsystems. For example, a change in the alignment of the TA does not influence the alignment of the MOT. That means better flexibility and less time in aligning in case changes or improvements are needed in one of the previous parts. In addition to that, the fiber provides some kind of filtering of the beam, spatial and spectral. This is very important in our case that we need a very good beam quality. In the following subsections, there is a comparison between the beam before and after the fiber. All the measurements use the double-pass configuration.

4.3.1 Coupling Efficiency

The following graph describes the power that results from the TA as a function of the injection power. The power has been measured at two points, just after the TA and after the optical fiber. As expected, we can see that we have losses in the power due to the shape of the beam. From this graph we can extract the coupling efficiency (fig.(4.22)). We can see that the coupling efficiency has a weak dependence on the injection power, because as we increase the injection power, the quality of the beam gets better (see fig.(4.19)), therefore the light coupled in the optical fiber increases. The coupling efficiency is about 50%.

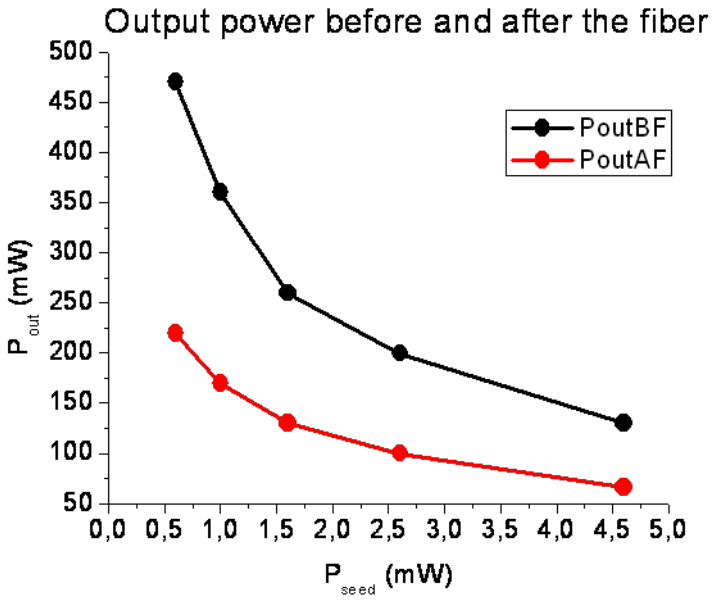

Figure 4.21: Power resulting from the TA, just after the TA (black line) and after the optical fiber (red line).

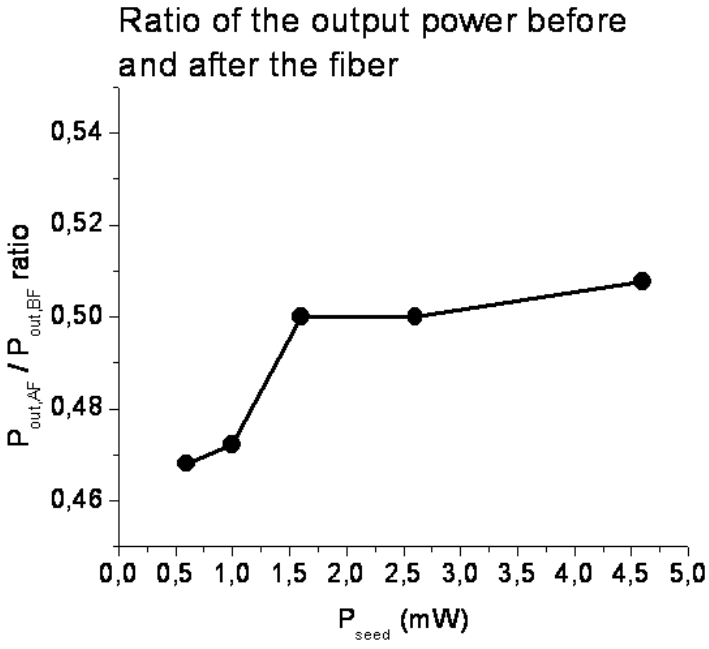

Figure 4.22: Ratio of the power before and after the optical fiber. We can see that the coupling efficiency in the fiber is almost 50%.

4.3.2 Spectral Filtering

In the following diagram (fig.(4.23)), there is a comparison between the ratio of the amplified light divided by the spontaneous emission coming from the TA, before and after the fiber as a function of the injection power for the single pass configuration.

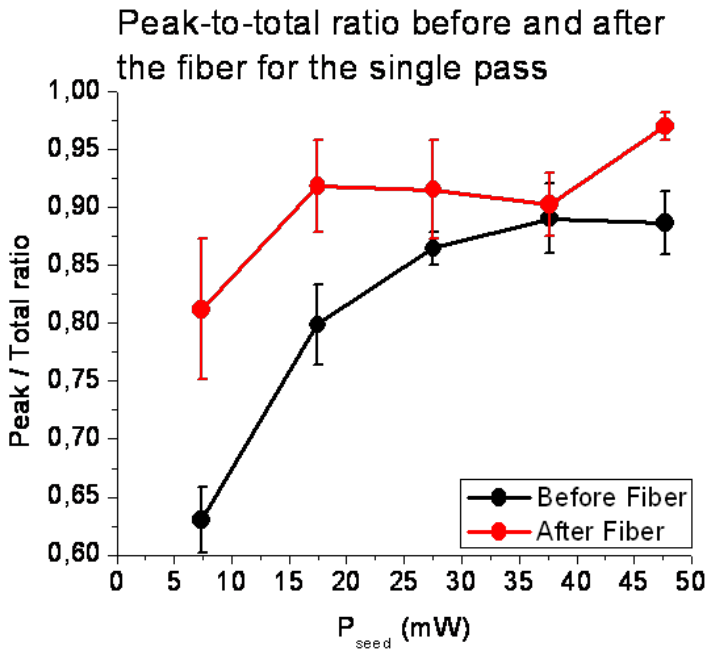

Figure 4.23: Peak-to-total ratio before and after the fiber. The measurements use the single pass case, though we expect the same behavior for the double pass configuration.

We can see that after the fiber, the ratio is higher, and hence the beam quality is better. This happens because the spontaneously emitted radiation contained in the background is spatially and temporally incoherent and thus cannot be effectively coupled in the fiber. As a result, the beam is filtered by the fiber.

4.3.3 Spatial Filtering

Apart from the spectral filtering that the optical fibers provide us, there is spatial filtering as well. In fig.(4.24) there are two photographs of the beam before and after the fiber, for comparison. It is clear that after the fiber the shape of the beam is vastly improved.

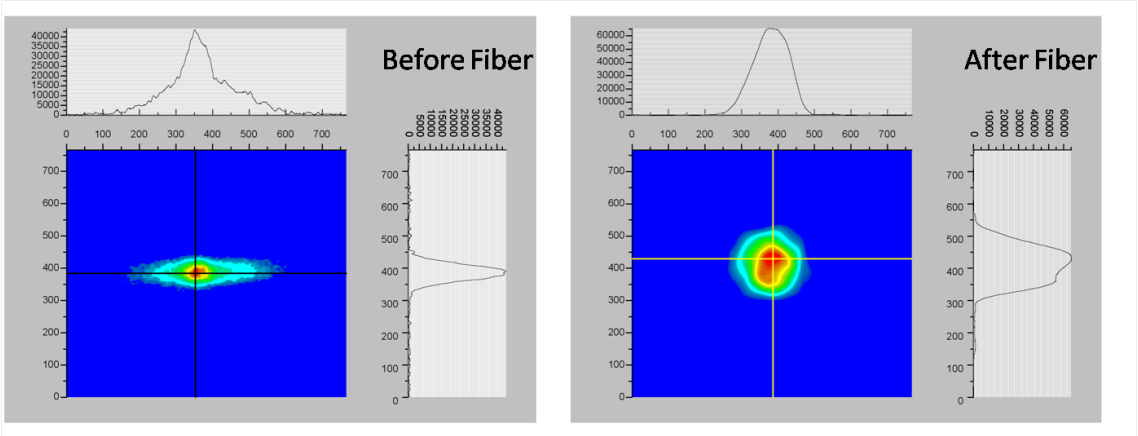

Figure 4.24: Profile of the beam before and after the fiber. It is clear that the quality of the beam improves greatly after the fiber.

4.4 Comparison between the Single Pass and the Double Pass Configurations

Since we have tried both kinds of configuration, the single and the double pass, we give some results for comparison. We see how the double pass is simpler and cheaper, as it does not need the use of an extra laser diode (slave laser) and, the most important, it needs much less injection light. In addition, as we operate the TA with less injection current, we expect a longer lifetime of the device.

Fig.(4.25) shows the graph with the output power versus the injection power for different injection power. From this graph we can find the threshold current of the device which is shown in fig.(4.26).

The output power as a function of P_{seed} for the single pass configuration is shown in fig.(4.27). The measurements were taken for different values of injection current. As it was expected, if we increase the P_{seed} or the current, the output power increases. The maximum output power is roughly $700mW$ for current equal to $2A$ and $P_{seed} = 50mW$. The corresponding maximum value for the double pass configuration is $P_{out} = 600mW$ for current equal to $1.6A$ and $P_{seed} = 0.4mW$. We can see that for the double pass configuration, we can have almost the same output power with 100 times lower injection power and less injection current.

In order to check the beam quality, we made a graph with the ratio of the amplified light and the total light emitted by the TA, for different values of injection current. This is shown in fig.(4.28).

The ratio does not depend on the current, since for all values of current the curves do not vary significantly. It does depend on the seeded power though since it increases while we increase the P_{seed}. It begins to be satisfactory for $P_{seed} \simeq 30mW$, while for the double pass configuration the corresponding value is $P_{seed} \simeq 0.5mW$.

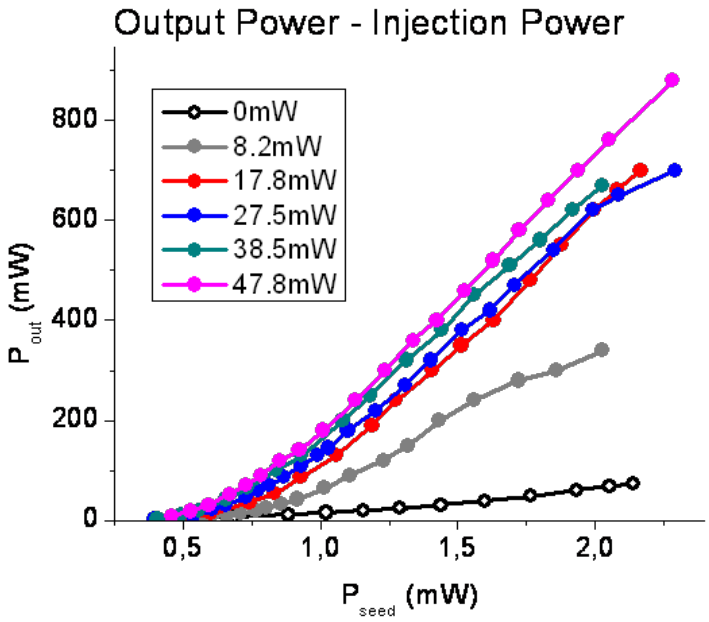

Figure 4.25: Output power versus injection current for different injection power for the case of the single pass.

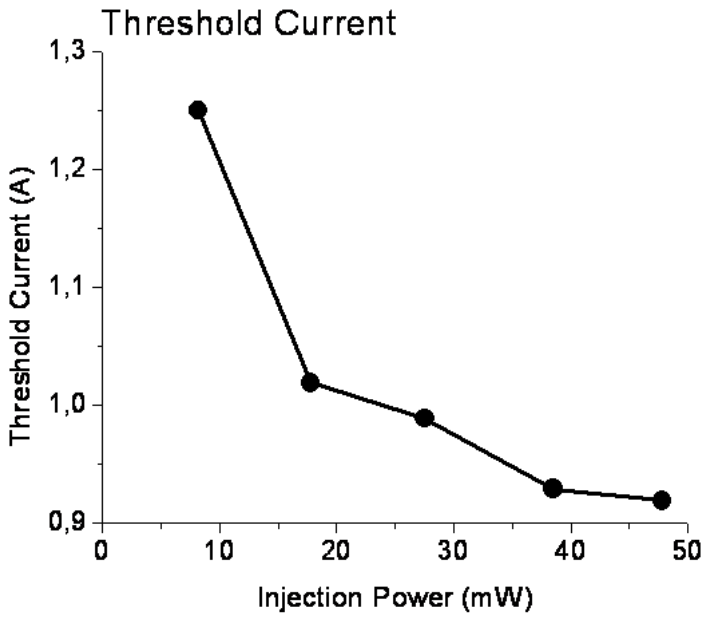

Figure 4.26: Change of the threshold current of the device for different injection power for the single pass configuration.

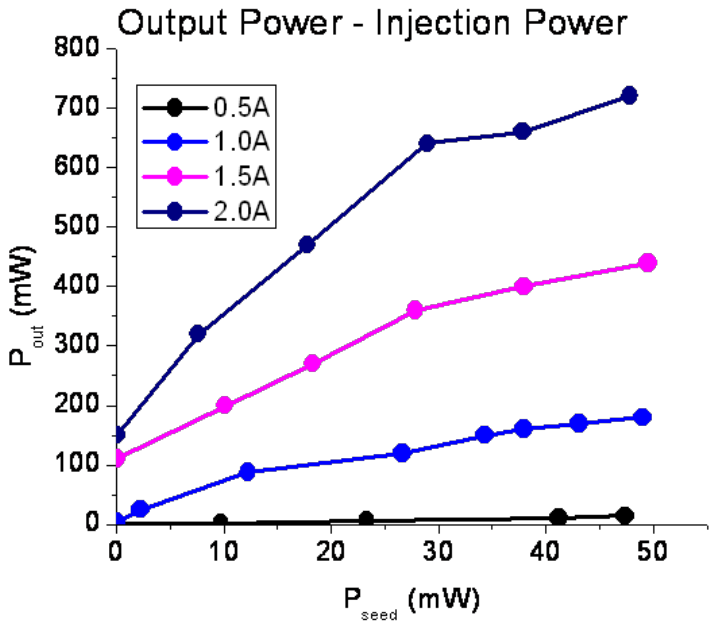

Figure 4.27: Output Power versus Injection Power for different injection current for the single pass case.

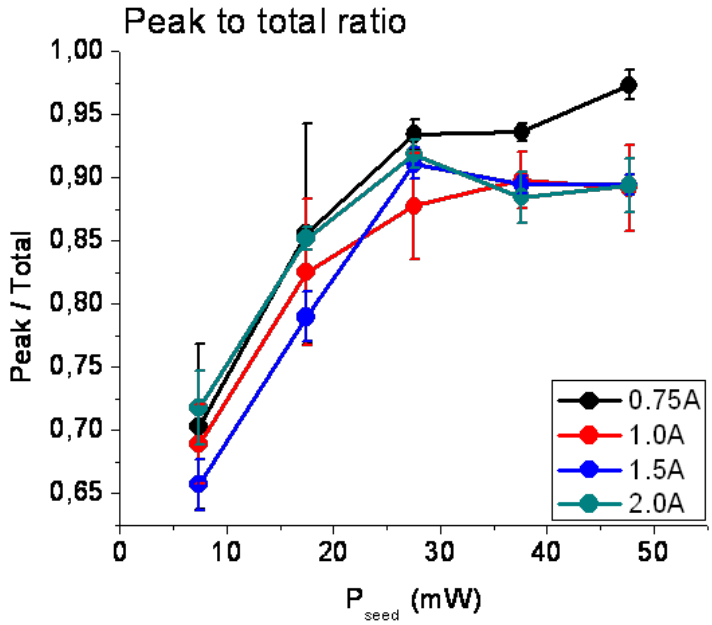

Figure 4.28: Peak to total ratio as a function of P_{seed} for different injection current for the single pass case.

Chapter 5

Conclusions

In conclusion, we built a stable, narrow linewidth laser system to be used for the creation and the observation of Bose-Einstein Condensates. It is more compact and cheaper comparing to the commercially available laser systems. Since many beams of different frequencies are needed for the several stages of the development of a BEC, we made the laser system frequency tunable, using a set of AOMs. In that way we cover all our needs for light using only two master lasers.

For the beams that need higher power, as for the case of the MOT beams, we built an amplification system much cheaper than the corresponding system available on the market, and also its demands on the seeding power are one hundred times lower. In addition, since we operate the amplifying device with lower current values, we can assure a longer lifetime of the device. The whole system is designed and built in such a way that can operate at a locked frequency for many hours, while it is stable enough that it does not need corrections in the alignment for months. That makes it a reliable system which is very important when we deal with a BEC, where everything must work perfectly.

Appendix A

Theory of Laser Diodes

The idea of using semiconductors for making lasers was first proposed in 1961. What was exactly proposed was to inject carriers in a p-n junction in order to cause stimulated emission, which is necessary in order for a device to lase. One year after, stimulated emission was observed in a simple GaAs p-n junction [11], and this opened the way to construct the first diode lasers.

Since then a lot of improvement has occurred. Diode laser technology uses many complex and, often, not very understood devices. Although their performance competes very well with that of the other kinds of lasers. In fact, diode lasers are a very compact and relatively cheap solution for experiments in many fields of science.

The output light of a diode laser can be a cw radiation of low or moderate power, or pulsed intense radiation with power of millions of Watts. The wavelength range that can be achieved covers a wide region of the spectrum (0.7 - 30 μm) Their linewidth is relatively broad, and that's why, in many cases, it needs to be locked to a certain frequency and stabilized.

A.1 Luminescence

If an excitation occurs in a solid, we may have radiation processes, called luminescence. There are several kinds of luminescence, depending on the kind of the excitation. For example, when the solid is excited optically, the process is called photoluminescence. But for the laser diodes, that we are interested in, the process that takes place is the electroluminescence, where the the emission of light is caused by imposing an electrical current through the material[12, 13, 14, 15].

If electrons from the valence band receive an appropriate amount of energy, they jump somewhere at the conduction band. Very rapidly, they cascade to the bottom of the conduction band emitting phonons. This process is very fast ($\sim$100 fs) comparing to the radiative lifetimes which are of the order of a nanosecond. That's why, they first fall to the minimum of the conduction band and then they recombine with the holes of the valence band emitting a photon. This photon of course has an energy very close to the energy of the gap of the material.

The number density of the electrons in the conduction band, is given by the

Fermi-Dirac statistics:

$$N_e = \int_{E_g}^{\infty} g_c(E) f_e(E) dE \tag{A.1}$$

where g_e is the density of states in the conduction band given by the equation

$$g_c(E) = \frac{1}{2\pi^2} \left(\frac{2m_e^*}{\hbar^2} \right)^{3/2} (E - E_g)^{1/2} \tag{A.2}$$

and $f_e(E)$ is the Fermi-Dirac distribution:

$$f_e(E) = \left[exp\left(\frac{E - E_F^c}{k_B T} \right) + 1 \right]^{-1} \tag{A.3}$$

In Eq.(A.3), E_F^c represents the quasi-Fermi level for the electrons of the conduction band, since we are not in equilibrium and there is not a unique Fermi level for the electrons and the holes.

If we combine eqns (A.2)-(A.3), we obtain a full expression for the number density of the electrons in the conduction band:

$$N_e = \int_0^{\infty} \frac{1}{2\pi^2} \left(\frac{2m_e^*}{\hbar^2} \right)^{3/2} E^{1/2} \left[exp\left(\frac{E - E_F^c}{k_B T} \right) + 1 \right]^{-1} dE \tag{A.4}$$

In exactly the same way, we can derive the number density of the holes of the valence band:

$$N_h = \int_0^{\infty} \frac{1}{2\pi^2} \left(\frac{2m_h^*}{\hbar^2} \right)^{3/2} E^{1/2} \left[exp\left(\frac{E - E_F^v}{k_B T} \right) + 1 \right]^{-1} dE \tag{A.5}$$

In eqns (A.4)and (A.5), we measure the energy relatively to the edges of the bands. So for the N_e we measure the energy upwards with the zero at the bottom of the conduction band, and for the N_h, we measure the energy downwards with the zero at the top of the valence band.

Einstein's A coefficient determines the spontaneous emission for transition between two levels.

$$\left(\frac{dN}{dt} \right)_{rad} = -AN \tag{A.6}$$

which has the solution:

$$N(t) = N(0) exp(-At) = N(0) exp(-t/\tau_R) \tag{A.7}$$

N(t) is the upper level population at time *t*, and $\tau_R = A^{-1}$ is the *radiative lifetime* of the transition.

In order to have emission, the high emission probabilities and the short radiative lifetimes are not enough. We have to have populated the upper level and empty the lower level. Eq.(A.8) gives the luminescent intensity at frequency ν:

$$I(h\nu) \propto |M|^2 g(h\nu) \times level\ occupancy\ factors \tag{A.8}$$

where the occupancy factors give the probabilities that the relevant upper level is occupied and the lower level is empty. M is the matrix element for the transition, and

$g(h\nu)$ is the density of states, which determine the quantum mechanical transition probability, given by Fermi's Golden Rule.

Now we can go back to eqns (A.4) and (A.5). Once we know these equations, we can compute the occupancy factors required to calculate the emission spectrum from eq.(A.8). To do that, we assume that we have low carrier densities and high temperature. Under this assumption, eq.(A.3) becomes

$$f(E) \propto exp\left(-\frac{E}{k_B T}\right) \tag{A.9}$$

and the emission spectrum becomes

$$I(h\nu) \propto (h\nu - E_g)^{1/2} exp\left(-\frac{h\nu - E_g}{k_B T}\right) \tag{A.10}$$

The first term comes from the density of states, and the second from the Boltzmann statistics of the electrons and holes. The spectrum described by eq.(A.10) looks like the spectrum shown in fig. A.1:

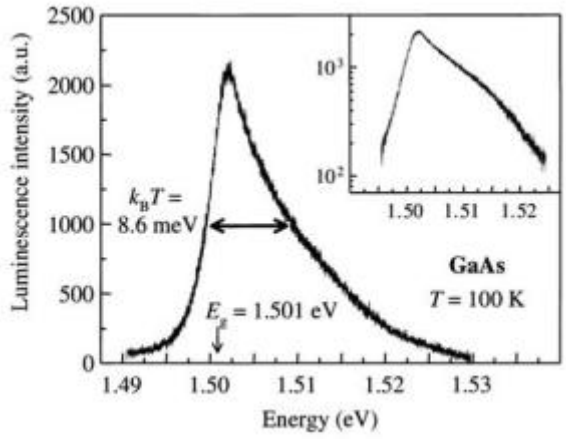

Figure A.1: Luminescence Spectrum of GaAs at 100K. The inset is the same plot in a logarithmic scale.

In the beginning it rises sharply at E_g, and then falls off exponentially with a decay constant $k_B T$. The width of the peak is again $\propto k_B T$.

Finally, we should mention the luminescent efficiency, η_R, which is given by:

$$\eta_R = \frac{AN}{N(1/\tau_R + 1/\tau_{NR})} = \frac{1}{1 + \tau_R/\tau_{NR}} \tag{A.11}$$

where $A = \tau_R^{-1}$. If η_R approaches to unity, then we have maximum amount of light emitted. That means that we need the radiative processes to have much shorter lifetime than this of the non-radiative processes ($\tau_R \ll \tau_{NR}$) in order to have emission.

A.2 Stimulated Emission

Electroluminescence, which is related to the spontaneous emission, is an important process in order for a laser diode to start its operation, but, as the name "laser" yields, the lasing procedure is based on the the stimulated emission. Stimulated emission causes an increase in the photon number as the light interacts with the atoms of the medium, which leads to optical amplification. Except the spontaneous and the stimulated emission, there is a third process that we should mention, which is the absorption, and causes beam attenuation. The transition rates are given by

$$\frac{dN_1}{dt} = -B_{12}N_1u(\nu) \tag{A.12}$$

$$\frac{dN_2}{dt} = -B_{21}N_2u(\nu) \tag{A.13}$$

for the absorption and the stimulated emission respectively. $N_1(t)$ and $N_2(t)$ are the populations in levels 1 and 2 respectively at time t, B_{12} and B_{21} are the Einstein coefficients for the corresponding processes, and $u(\nu)$ is the energy density of the electromagnetic wave at frequency ν, that interacts with the atoms. When the system is at thermal equilibrium, the lower level population, N_1 will be greater than that of the higher level, N_2, and their ratio will be given by Boltzmann's law:

$$\frac{N_2}{N_1} = \frac{g_2}{g_1}exp\left(-\frac{h\nu}{k_BT}\right) \tag{A.14}$$

where g_1 and g_2 are the degeneracies of levels 1 and 2 respectively.

N_1 greater than N_2, means net attenuation of the beam. In order to make the stimulated emission process to dominate over absorption, and thus have net amplification of our beam, we need $N_2 > N_1$. This condition is called *population inversion*.

Another characteristic of a laser is its cavity. In fig.(A.2) we show a schematic diagram of the laser cavity. A cavity requires mirrors, and in the case of semicon-

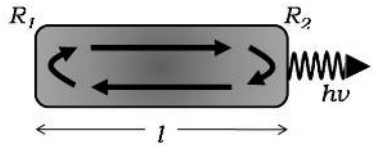

Figure A.2: Laser cavity of length l. R_1 and R_2 are the mirror reflectivities.

ductor lasers, the role of the mirrors plays the interface between the semiconductor and the air, which, because of the difference in the refractive index, reflects the light. The reflectivities are of the order of 30%, although they can be higher or lower with the aid of spacial coatings. For the followings, we assume the reflectivities of the two sides of the material, R_1 and R_2, different and that $R_1 \gg R_2$.

In the cavity, the light produced by electroluminescence is reflected back and forth, and gets amplified by the process of stimulated emission, given that we have

population inversion between the conduction and valence bands. For a specific value of the injection current I_{in}, which is called *threshold current* I_{th}, the laser starts to oscillate. The spectrum of the emission will be defined by the cavity, as only the resonant modes to the cavity will be amplified. The condition that the resonant modes must satisfy is

$$m\frac{\lambda_n}{2} = l, \qquad m = integer \tag{A.15}$$

where λ_n is the wavelength inside the semiconductor, and is equal to λ_0/n, with λ_0 the wavelength in the air and n the refractive index of the semiconductor. Eq.(A.15) in terms of the frequency, becomes

$$\nu = m\frac{c}{2nl} \tag{A.16}$$

In the cavity there are losses because of the radiation that exits the cavity through the mirrors, or because of other processes, such as scattering losses or impurity absorption in the medium. In order to have stable laser oscillation, the gain must exactly balance the losses. This condition is described by

$$R_1 R_2 e^{2\gamma_\nu l} e^{-2\alpha_b l} = 1. \tag{A.17}$$

γ_ν is the incremental gain coefficient and α_b the attenuation coefficient. The factor of 2 in the exponentials is due to the fact that the light passes twice through the medium during a round trip. This condition defines the threshold gain, γ_{th}, required to have laser oscillation:

$$\gamma_{th} = \alpha_b - \frac{1}{2l} ln(R_1 R_2) \tag{A.18}$$

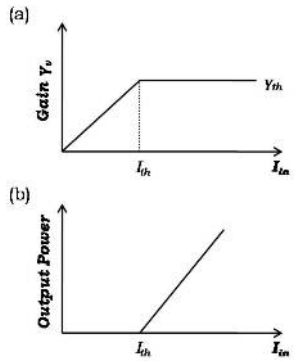

Figure A.3: (a) Gain coefficient γ_ν and (b) output power as a function of injection current I_{in}.

As can be seen in fig.A.3(a), the gain coefficient increases linearly with the injection current, until it reaches the maximum value γ_{th}, defined by eq.(A.18), and then it stays constant as the stability condition (A.17) demands. This is the point that the laser starts to oscillate. The output power, P_{out}, for $I_{in} > I_{th}$ can be written as

$$P_{out} = \eta\frac{h\nu}{e}(I_{in} - I_{th}) \tag{A.19}$$

where η is the quantum efficiency and defines the fraction of the electron-hole pairs that recombine radiatively. η can be determined by the slope of the graph of fig.A.3(b):

$$slope = \frac{P_{out}}{I_{in} - I_{th}} = \frac{\eta h\nu}{e} \tag{A.20}$$

Bibliography

[1] K.B.Davis, M.O.Mewes, M.R.Andrews, N.J.van Druten, D.S.Durfee, D.M.Kurn, and W.Ketterle. Bose-einstein condensation in a gas of sodium atoms. *Physical Review Letters*, 75:3969–3973, 1995.

[2] M.H.Anderson, J.R.Ensher, M.R.Matthews, C.E.Wieman, and E.A.Cornell. Observation of bose-einstein condensation in a dilute atomic vapor. *Science*, 269:198–201, 1995.

[3] H.Smith C.J.Pethick. *Bose-Einstein Condensation in Dilute Gases*. Cambridge, 2002.

[4] H.J.Metcalf and P.van der Straten. *Laser cooling and Trapping*, volume 70. Springer, 1999.

[5] C.J.Foot. *Atomic physics*. Oxford University press, 2005.

[6] S.Chu, L.Hollberg andJ.E.Bjorkholm, A.Cable, and A.Ashkin. Three-dimensional viscous confinement and cooling of atoms by resonance radiation pressure. *Phys. Rev. Lett.*, 55:48–51, 1985.

[7] K.Liu and M.G.Littman. Novel geometry for single-mode scanning of tunable lasers. *Optics Letters*, 6:117–118, 1981.

[8] J.N.Walpole. Semiconductor amplifiers and lasers with tapered gain regions. *Optical and Quantum Electronics*, 28:623–645, 1996.

[9] H.Ghafouri-Shiraz and P.W.Tan. Study of a novel laser diode amplifier structure. *Semicond. Sci. Technol.*, 11:14431449, 1996.

[10] D.Voigt. Characterization of a high-power tapered semiconductor amplifier system. *Appl. Phys. B*, 72:279–284, 2001.

[11] R.N.Hall, G.E.Fenner, J.D.Kingsley, T.J.Soltys, and R.O.Carlson. Coherent light emission from gaas junctions. *Physical Review Letters*, 9:366369, 1062.

[12] M.Fox. *Optical properties of solids*. Oxford University press, 2001.

[13] R.Diehl. *High-Power Diode lasers*. Springer, 2000.

[14] S.L.Chuang. *Physics of Optoelectronic Devices*. John Wiley & Sons, 1995.

[15] O.Svelto. *Principles of Lasers*. , 2nd edition, 1986.

Index